DIMENSIONAL CHANGES AND STRAIN ANALYSIS OF PRO-ROOT WHITE MINERAL TRIOXIDE AGGREGATE, ENDOSEQUENCE ROOT REPAIR MATERIAL-FAST SET PUTTY, AND BIODENTINE DURING SETTING

A THESIS

SUBMITTED TO THE FACULTY OF

UNIVERSITY OF MINNESOTA

BY

KRISTINE ASHLEIGH KNOLL

IN PARTIAL FULFILLMENT OF THE REQUIREMENTS

FOR THE DEGREE OF

MASTER OF SCIENCE

DR. SCOTT MCCLANAHAN, DR. ALEX FOK, DR. SAMANTHA ROACH

SEPTEMBER 2017

ACKNOWLEDGEMENTS

I would like to thank my advisor and mentor, Dr. Scott McClanahan, for your incredible support throughout this process and encouraging me to take risks. I am the product of your dedication and support.

Also, I would like to thank some creative faculty members and colleagues who had an influence this study: Dr. Alex Fok, Dr. Samantha Roach, Dr. Carolyn Primus, Yeung Ho, Mike Hanson, and Simona Ivanov.

DEDICATION

To health, wealth and hoppiness 

TABLE OF CONTENTS

LIST OF TABLES

APPENDIX

LIST OF FIGURES

INTRODUCTION

An important prognostic factor influencing treatment outcomes of apical surgeries in endodontics is the selection of an appropriate root-end filling material. The emergence of new generations of calcium-silicate based root-end filling materials has, together with the introduction of the modern microsurgical technique, contributed to better clinical outcomes compared to traditional retrograde treatment strategies. And the by-products formed during the hydration reactions of calcium-silicate based materials contribute to this material's bioactivity. The physical, chemical, and biological properties of the prototypical 'modern' root-end filling materials have been investigated by many *in vitro* studies, and production of any new retrograde filling materials are commonly compared against the first proposed calcium-silicate based root-end filling material, mineral trioxide aggregate (MTA). ProRoot MTA™ (Denstply Tulsa Dental Specialities, Johnson City, TN) was the first commercially available form of MTA and has been formulated as a tooth-colored variety, ProRoot White MTA, to overcome reported disadvantages of the gray variety. Similar to the properties of ProRoot MTA, newer generations of retrograde materials have been introduced as appropriate alternatives, such as Biodentine™ (Septodont, Cambridge, ON, Canada) and Endosequence Root Repair Material ™ (Brassler, Savanah, GA). In the presence of periapical tissue fluid, dimensional stability of retrograde materials is both necessary for producing an adequate apical seal and an ideal properties of root-end filling materials (Kim, Pecora, & Rubinstein, 2001). Theoretically, the absence of a material's marginal adaption or adhesion to the root canal dentinal surface may contribute to persistent apical disease. The microscopic and macroscopic shrinkage of root-end filling materials may produce an inadequate seal by creating gaps and channels that allow the egress of bacterial and their irritants into the periapical tissue. Whereas microscopic expansion of these materials may improve the seal, macroscopic expansion may induce fractures of the root-end and therefore serve as a portal of entry for re-contamination.

The physical properties of root-end filling materials should be in compliance with the standards and specifications for testing of endodontic cements or sealers. In compliance with the International Standard 6876 (ISO 6876:2001) and specification number 57 from the American National Standard Institute/American Dental Association (ANSI/ADA No. 57:2000) standards for testing the dimensional stability of endodontic sealers, the mean linear shrinkage and expansion should not exceed 1% and 0.1% after 30 days, respectfully. Under the required 1% maximum shrinkage, a material thickness of 100 μm can be allowed 1 μm of displacement, and, as such, a void of this size is sufficient enough for bacterial penetration and colonization. Compared to 0.1% expansion of similar thickness, the allotted displacement of 0.01 μm may not be possible to detect with the instrument's sensitivity specified in ISO 6876:2001 and ANSI/ADA No. 57:2000 testing standards. In addition to sensitivity, other limitations of these testing methods include the sample preparation sizes, use of restrained molds, environmental testing conditions, instrument's measurement range, and recordings made in the vertical direction only. In order to overcome these drawbacks, various measuring instruments and testing techniques have been investigated for improving the accuracy of quantifying the dimensional changes under simulated *in vivo* conditions. Contact instruments, such as a digital caliper or linear variable displacement transducer (LVDT), measure displacements on a single-point made on the material's surface and are invasive in nature. Whereas, digital image correlation (DIC) is a non-invasive instrument that uses an imaging recognition technique to optically track the movement of multiple reference points and has the potential to be used for measuring displacement during setting in root-end filling materials. The aim of this *in vitro* study was to evaluate the unrestricted dimensional change in the horizontal direction of ProRoot White Mineral Trioxide Aggregate, Endosequence Root Repair Material-Fast Set Putty and Biodentine in the horizontal axis during setting using the DIC technique.

REVIEW OF LITERATURE

Along with our patient's treatment preferences, the commitment towards integrating the best available evidence as part of our clinical decision-making process is the accepted standard of care in health care. Selecting an appropriate treatment option requires integrating the input from our patient's values and their ability to understand the treatment's prognosis, risks, and benefits based on our clinical knowledge and skills. Through the advancements made in our clinical armamentarium and through our greater understanding of both the etiology of persistent disease and apical healing, endodontic therapies are predictable treatment alternatives that can address our patient's desires to preserve their natural dentition. In contrast to extractions or prosthodontic replacement therapies, the aim of endodontic therapy is to prevent or treat apical periodontitis.

Studies have shown that apical periodontitis is fundamentally caused by a bacterial infection of the root canal system (Kakehashi, Stanley, & Fitzgerald, 1985; Moller, Fabricius, Dahlen, Ohman, & Heyden, 1981), while the radiographic presentation of radiolucency largely results from an immunological response from the egress of bacterial toxins and by-products into radicular tissue (Torabinejad, Eby, & Naidorf, 1985). Therefore, the objectives of non-surgical root canal therapy are to chemo-mechanically eliminate these intraradicular irritants and to three-dimensionally seal the root canal system from any residual or potential irritants from the root canal system (Schilder, 1967, 1974). Due to the complex and highly variable morphology of the root canal system and our subsequent inability to guarantee complete disinfection and debridement in 100% of cases, non-surgical (orthograde) root canal therapies alone may not be sufficient in addressing and eliminating the etiology. Patients should be informed that the probability of complete healing following initial root canal treatment is 86% (de Chevigny et al., 2008), and that endodontic treatments for managing persistent or emergent infections may include orthograde retreatments and apical surgeries, retrograde approach. In cases where persistent infection are due to inadequacies in the quality of obturation or a missed canal, the bacterial

populations present may resemble those of a primary infection and are, therefore, considered less resistant (Sundqvist & Figdor, 2003). Under these circumstances, orthograde retreatments showed a 36% increase in success compared to a well-obturated canal (de Chevigny et al., 2008). Despite these non-surgical efforts, the presence of persistent disease may also be contributed by the presence of extraradicular infections, foreign-body reactions, cysts, or extruded endodontic materials (Nair, 2004). When considering the risks and benefits of treating persistent disease, the presence of a large post or separated instrument may contraindicate using such orthograde approaches and the inability to further disinfect the root canal system may require surgical intervention (Kim et al., 2001). Thus, the decision to treat post-endodontic treatment failures, non-surgically or surgically, pose many clinical challenges and our patients should be informed that the chances of healing are 82% (de Chevigny et al., 2008) and 74% (Barone, Dao, Basrani, Wang, & Friedman, 2010), respectively.

Apical surgery is a retrograde procedure that consists of a root-end exposure, resection, preparation, and filling. Recent advancements in techniques have transformed apical surgery into a microsurgical procedure (Kim & Kratchman, 2006). The modern microsurgical techniques differ from the traditional approach in that it incorporates the use of magnification and illumination, CBCT imaging, micro-instrumentation, and bioactive root-end filling materials (Kim & Kratchman, 2006). In contrast, the traditional surgical technique required the use of larger osteotomy preparations, increased bevel angles, root-ends prepared with burs, and less superior retrograde materials such as amalgam or intermediate restorative material (IRM) (Kim & Kratchman, 2006). In a study by Tsesis (2006), the authors reported a higher surgical success rate using the modern approach compared to the traditional, 91.1% and 44.2% respectively.

In the modern microsurgical technique, a 3mm apical resection is considered optimal to remove the greatest number of lateral canals, isthmus and ramifications (Kim et al., 2001). The indications for preparing a class 1 root-end cavity to a depth of 3mm, using diamond or zirconium

coated ultrasonic tip, include 1) eliminating persistent intraradicular irritants, 2) removal of pre-existing obturation material, and 3) creating space to accommodate root-end filling materials (Carr, 1997). The rationale for filling the root-end cavity preparation with a material relates to our inability to sufficiently shape, debride, and seal such a complex system in each and every patient (Friedman, 1991). Consequently, the objective of a retrograde filling material is to provide an antibacterial and fluid tight seal, to prevent recontamination after the ramifications and lateral canals have been resected and the root-end prepared (Friedman, 1991). The composition of root-end filling materials has been cited as an important intraoperative variable associated with outcome measures of surgical endodontic treatment (Friedman, 2005). Specifically, the most important material-related factor affecting treatment outcome is the material's ability to form a fluid tight seal, trap intracanal bacteria, their by-products, and preventing toxic substances from reaching the periapical tissue (Kim et al., 2001).

The evidence accumulated from numerous *in vitro* and *in vivo* studies suggest that a clinician's selection of retrograde material may affect the healing environment and surgical outcome. It is perhaps not surprising, then, that traditional retrograde materials (amalgam, zinc oxide eugenol cements, composite resin, and GI and polycarboxylate cements) have fallen out-of-favor in recent decades (Torabinejad & Pitt Ford, 1996; von Arx, Penarrocha, & Jensen, 2010). This trend is probably related to the relative superiority of newer products, which come closer to meeting the requirements for an 'ideal' root-end filling material as follows: biocompatibility, non-toxic, bacteriostatic, non-resorbable, radiopaque, excellent working properties, non-staining, adherent to teeth, dimensionally stable over time and promoting of cementogenesis (Kim et al., 2001; Torabinejad & Pitt Ford, 1996). In a literature review of existing retrograde materials, investigators have supported the use of MTA due to its superior sealing ability (Torabinejad, Hong, McDonald, & Pitt Ford, 1995; Torabinejad & Parirokh, 2010), compressive strength (Torabinejad, Hong, et al., 1995), solubility (Herzog-Flores, Andrade, & Mendez, 2000),

antibacterial effects (Parirokh & Torabinejad, 2010), biocompatibility (Torabinejad & Parirokh, 2010), and cementum formation (Roberts, Toth, Berzins, & Charlton, 2008; Torabinejad & Parirokh, 2010) compared to IRM, amalgam, and SuperEBA (Torabinejad & Pitt Ford, 1996).

Introduced in 1993 by investigators at Loma Linda University, Mineral Trioxide Aggregate (MTA) is a hydrophilic powder mix of American Standards for Testing Materials (ASTM) type 1 Portland cement mixed 4:1 with radiopacifier (Torabinejad, Hong, et al., 1995). Portland cement is primarily composed of tricalcium silicate ($3CaO \cdot SiO_2$), dicalcium silicate ($2CaO \cdot SiO_2$), tricalcium aluminate ($3CaO \cdot Al_2O_3$), and tetracalcium aluminoferrite ($3CaO \cdot Al_2O_3 \cdot Fe_2O_3$) and the powder mix is produced by firing three oxides in a kiln: calcia (CaO), silica (SiO_2), and alumina (Al_2O_3) (De Deus, Camilleri, Primus, Duarte, & Bramante, 2014). The first commercially available form of MTA was ProRoot MTA™ (Denstply Tulsa Dental Specialities, Johnson City, TN) and is available in two varieties, "gray" and "white". According to the material safety data sheet (MSDS), ProRoot White MTA™ (W-MTA) is composed of 75% Portland cement, 20% bismuth oxide (Bi_2O_3), and 5% calcium sulfate dihydrate (gypsum, $CaSO_4 \cdot 2H_2O$) by mass as seen in Table 1 (MSDS, 2002). Rietvald X-ray diffraction (XRD) analysis identified the composition of un-hydrated W-MTA to contain a similar composition to that of Portland cement, with the exception of bismuth oxide and tetracalcium aluminoferrite (Table 1) (Belio-Reyes, Bucio, & Cruz-Chavez, 2009). Compared to its white counterpart, ProRoot Gray MTA™ (G-MTA) contains tetracalcium aluminoferrite (Parirokh & Torabinejad, 2010) and this mineral oxide, along with compounds like bismuth oxide, contributes its higher potential for tooth discoloration (Asgary, Parirokh, Eghbal, & Brink, 2005).

Camilleri (2007) investigated the setting characteristics of MTA and Portland cements, which involve the formation of calcium hydroxide ($Ca(OH)_2$) and calcium silicate hydrate

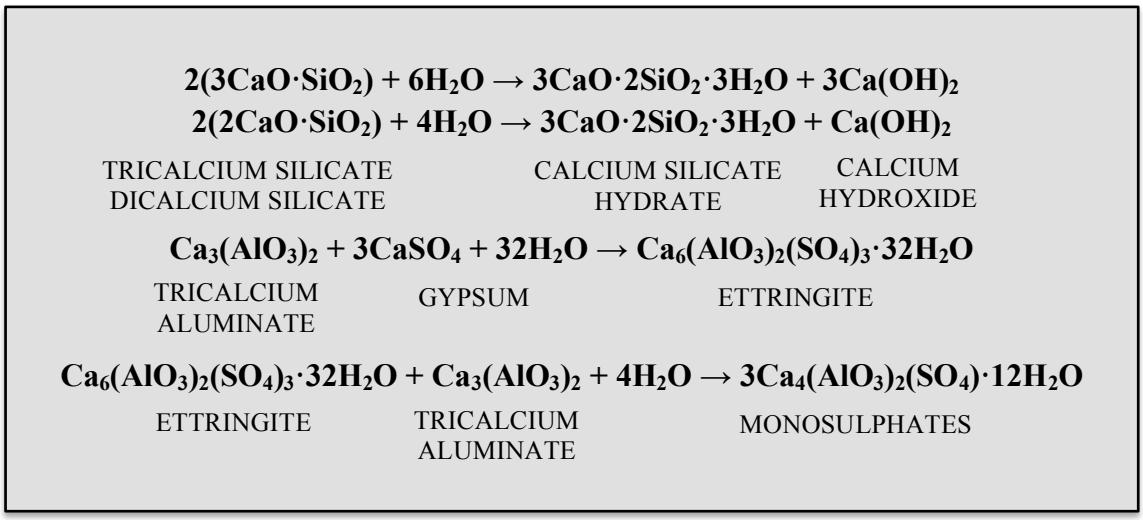

Figure 1: The hydration reactions of tri- and dicalcium silicates, tricalcium aluminate and gypsum in MTA and Portland cement.

($3CaO \cdot 2SiO_2 \cdot 3H_2O$) under two hydration reactions shown in Figure 1. The hydrolysis of tri- and dicalcium silicates form the colloidal gel-like phase (calcium silicate hydrate) and this by-product is responsible for the strength in the material (Camilleri, 2007). The release of calcium ions (Ca^{2+}) and hydroxyl ions (OH^-) form the crystalline phase (calcium hydroxide), which is related to the material's solubility and mineralization capacity (Camilleri, 2007; Sarkar, Caicedo, Ritwik, Moiseyeva, & Kawashima, 2005). Additionally, the latter by-product is responsible for the production of an alkaline environment capable of deprotonating the calcium silicate hydrate and these negative charges act as nucleation sites for calcium hydroxide crystals deposits (Camilleri, 2007; Gandolfi, Taddei, Tinti, & Prati, 2010). Phosphate ions (PO_4^{2-}) present in the apical tissue

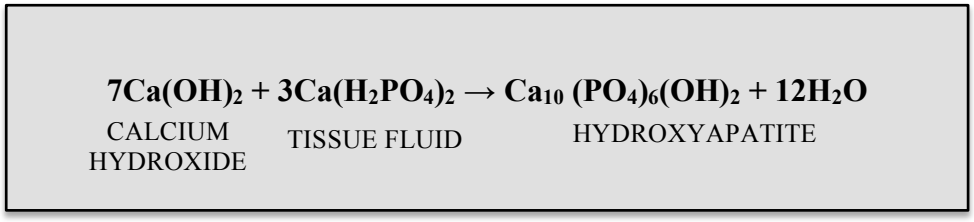

Figure 2: The precipitate formed in the presence of tissue fluid.

fluids will also attract calcium hydroxide and this eventually leads to the precipitation of hydroxyapatite crystals ($Ca_{10}(PO_4)_6(OH)_2$) (Gandolfi et al., 2010; Sarkar et al., 2005) (Figure 2). XRD analysis by Sarkar et al. (2005) showed apatite formation of MTA when immersed in a phosphate-buffered saline (PBS) solution after 3 days. Formation of apatite was subsequently proven using ProRoot MTA (Gandolfi et al., 2010), tricalcium-silicate based cements (Liu & Chang, 2009), modified dicalcium-silicate based cements (Chen, Ho, Chen, Wang, & Ding, 2009; Ding, Shie, & Wang, 2009) and Portland cement immersed in phosphate-containing solutions (Coleman, Awosanya, & Nicholson, 2009). Bioactivity of calcium-silicate based materials is related to this apatite-forming ability (ISO 23317, 2014) and contributes to the biological aim of apical surgery, which is to promote a favorable environment conducive for the regeneration of the hard- and soft-tissues (Kim et al., 2001). In a prospective outcome study by Saunders et al. (2008), the authors reported the radiographic and clinical healing of W-MTA to be 88.8%, with a mean follow-up period of 18 months.

According to the MSDS, ProRoot MTA should be manually mixed using a metal spatula on a glass slab for one minute in order to hydrate all powder particles in a 3:1 liquid proportion (MSDS, 2002; Torabinejad & Parirokh, 2010). If a longer working time is needed, the material should be covered with a moistened gauze in order to prevent evaporation (MSDS, 2002). During the hardening process, crystalline deposits of MTA eventually form an impermeable barrier (Camilleri, 2007, 2008) and this process can occur in approximately 3-4 hours (Dammaschke, Gerth, Zuchner, & Schafer, 2005; Ha, Bentz, Kahler, & Walsh, 2017; Torabinejad, Hong, et al., 1995), reaching a pH similar to that of calcium hydroxide (12.5) (Torabinejad, Hong, et al., 1995). Compared to Portland cement, bismuth oxide is present in the calcium silicate hydrate phase of MTA (Camilleri, 2007, 2008) and has been shown to increase its porosity and decrease compressive strength (Coomaraswamy, Lumley, & Hofmann, 2007). The size of the powder particles in W-MTA is generally smaller compared to G-MTA

Powder	MSDS	Rietvald XRD Analysis[a]
tricalcium silicate, $(CaO)3 \cdot SiO_2$	75%	51.9%
dicalcium silicate, $(CaO)2 \cdot SiO_2$		23.2%
tricalcium aluminate, $(CaO)3 \cdot Al_2O_3$		3.8%
tetracalcium aluminoferrite, $4CaO \cdot Al_2O_3 \cdot Fe_2O_3$		
calcium sulfate dehydrate (gypsum) $CaSO_4 \cdot 2\ H_2O$	5%	
calcium sulfate anhydrite, $CaSO_4$		1.3%
bismuth oxide, Bi_2O_3	20%	19.8%
Liquid		
distilled water, H_2O	100%	100%

Table 1: ProRoot White MTA (Denstpyl Tulsa Dental Specialities, Johnson City, TN) chemical composition. Rievald XRD Analysis[a] according to Belio-Reyes et al. (2009), photograph courtesy of Zedler (2016)

(Komabayashi & Spångberg, 2008), ranging from less than 1 to 30 μm (Parirokh & Torabinejad, 2010). The clinical significance of particle size relates to the material's handling properties (Kogan, He, Glickman, & Wantanabe, 2006) and potential to undergo hydraulic reactions (Belio-Reyes et al., 2009; Bentz et al., 2001). The long-setting time, early wash-out potential, tooth discoloration, and the handling properties are clinical disadvantages for using ProRoot MTA as a root-end filling material (Kogan et al., 2006; Lee, 2000). As such, newer formulations of calcium-silicate based materials have been developed in order to overcome these aforementioned limitations of ProRoot MTA.

Biodentine™ (Septodont, Cambridge, ON, Canada) is available in a powder-liquid formulation, where the powder is composed of tri- and dicalcium silicates, calcium carbonate ($CaCO_3$) and oxides (CaO), zirconium oxide (ZrO_2), and iron oxides (FeO) and the liquid contains calcium chloride ($CaCl_2$) and hydrosoluble polymer (Table 1) (MSDS, 2010). Rietvald X-ray diffraction (XRD) analysis identified the composition of un-hydrated Biodentine to contain no added dicalcium calicate or calcium oxide, (Table 2) (Camilleri, Sorrentino, & Damidot, 2013). Compared to the liquid component of MTA, calcium chloride is an accelerator added to

Powder	MSDS	Rietvald XRD Analysis[a]
tricalcium silicate, $(CaO)3 \cdot SiO_2$	>70%	80.1%
dicalcium silicate, $(CaO)2 \cdot SiO_2$	<15%	
iron oxide, FeO	<1%	
calcium oxide, CaO		
calcium carbonate, $CaCO_3$	>10%	14.9%
zirconium oxide, ZrO_2	5%	5.0%
Liquid		
distilled water, H_2O		
calcium chloride, $CaCl_2$	>15%	
hydrosoluble polymer		

Table 2: Biodentine (Septodont, Cambridge, ON, Canada) chemical composition. Rievald XRD Analysis[a] according to Camilleri et al. (2013), photograph courtesy of Zedler (2016)

increase the setting time and rate of strength, whereas the hydrosoluble polymer is used as a water-reducing agent (Septodont, 2010). Compared to ProRoot MTA, the clinical advantages of using Biodentine are the manufactured shorter setting time, 12 minutes, and similar compressive strength to dentin, 275-300 MPa (Craig & Peyton, 1958; Septodont, 2010). However, these values are not consistent with the study by Grech et al. (2013), where the authors reported a final setting time of 45 minutes and compressive strength of 67.15 MPa, after 28 days. Additionally, Biodentine exhibits a finer particle size (Camilleri, Sorrentino, et al., 2013) compared to MTA, and the presence of calcium carbonate in the powder enhances the hydraulic production of calcium hydroxide (Camilleri, Kralj, Veber, & Sinagra, 2012; Grech, Mallia, & Camilleri, 2013). According to the MSDS instructions for mixing, a capsule, containing a present quantity of 0.7 g powder is combined with 0.18 mL liquid and triturated for 30 seconds, which produces a more homogenous mix compared to hand mixing (MSDS, 2010). When Biodentine is used as a root-end filling material, excessive waste is inevitable due to the actual cavity volume prepared and the manufacturer's bulk packaging. As such, one of the advantages for developing a premixed calcium silicate material is to maintain the benefits of a homogenous consistency.

Endosequence Root Repair Material ™ (ERRM,Brassler, Savanah, GA) is a premixed product primarily composed of tri- and dicalcium silicates, zirconium oxide, tantalum pentoxide (Ta_2O_5), and calcium sulfate anhydrate ($CaSO_4$) (Table 3) (MSDS, 2014). To facilitate the ease of application, ERRM is commercially available in both a condensable putty or paste form dispensed in a syringe. ERRM-Fast Set Putty™ (ERRM-FS) is a second-generation putty preloaded into a syringe with a manufactured setting time of 20 minutes (MSDS, 2014). Rietvald X-ray diffraction (XRD) analysis identified the composition of un-hydrated ERRM-FS to contain no added calcium sulfate or tantalum (Table 3, Primus, 2017). Materials containing tantalum oxide and zirconium oxide produce more color stability compared to materials containing bismuth oxide, like MTA (De Deus et al., 2014). Like Biodentine, ERRM products report

approximately half of the particles being nano-sized (1 x 10^{-3} µm) compared to MTA, which has a lower surface-to-volume ratio for hydraulic reactivity (De Deus et al., 2014). According to the MSDS, ERRM- Putty™ (ERRM-P) has a working time of 30 minutes and the available moisture present in dentin initiates a final setting time of 4 hours (MSDS, 2014). However in a cytotoxic study by Damas et al. (2011), complete setting was exhibited in ERRM-P samples after 168 hours in 100 % relative humidity and in a pH study by Hansen et al. (2011), complete cure of this material was between 24 hours and 1 week, as evident by decrease in pH values. Ma et al. (2011) showed calcium carbonate precipitation on the surface of ERRM-P in the presence of air-drying, due to the reaction with carbon dioxide (CO_2) present in air. Therefore, the bioactivity of ERRM under *in vivo* conditions may not be reflective *in vitro* due to the absence of forming

Powder	MSDS	Rietvald XRD Analysis[a]
tricalcium silicate, $(CaO)3 \cdot SiO_2$	30-36%	38.3%
dicalcium silicate, $(CaO)2 \cdot SiO_2$	9-13%	24.4%
tantalum pentaoxide, T_2O_5	12-15%	
calcium sulfate anhydrate, $CaSO_4$	3-8%	
zirconium oxide, ZrO2	15-18%	26.9%

Table 3: ERRM-FS (ERRM,Brassler, Savanah, GA) chemical composition. Rievald XRD Analysis[a] according to Primus (2017), photography courtesy of Zedler (2016)

hydroxyapatite in various studies (Ma, Shen, Stojicic, & Haapasalo, 2011; Moinzadeh, Portoles, Wismayer, & Camilleri, 2016). However, in a private practice retrospective study by Shinbori *et al.* (2015), the authors reported the clinical and radiographic healing using ERRM-P to be 92%. In a histological animal study by Chen et al. (2015), ERRM-P was associated with a superior healing response and significantly more cementum-like and PDL-like tissue compared to G-MTA.

As mentioned previously, calcium silicate based materials undergo two hydration reactions during setting, and the formation of their by-products are responsible for the material's frequent use in modern apical surgeries (Figure 1). Using models to replicate *in vivo* conditions, many *in vitro* studies have aimed to describe the physical, chemical, and biological properties of these bioactive materials. The purpose for placing a root-end filling material is to produce an apical seal. One of the characteristics of an ideal root-end filling material is to be dimensionally stable over time when contacting periapical tissue fluids (Kim et al., 2001). An inadequate apical seal can create both a portal of entry and exit of intracanal irritants, which may contribute to persistent apical disease. Microscopic or macroscopic shrinkage of these materials can provide residual bacteria with a continued supply of nutrients, and the diffusion of their by-products into the periapical tissue can maintain an inflammatory response (Torabinejad et al., 1985). Microscopic expansions of root-end filling materials can, theoretically, have the advantage of producing a tighter apical seal; however, macroscopic expansion may counteract this purpose if the materials induce fractures. In a study by Weller et al. (2008), the authors concluded that the formation of hydroxyapatite may further improve the material's sealing ability, and this was subsequently shown by slight expansion of calcium-silicate based materials in a study by Gandolfi et al. (2009). *In vitro* bacterial leakage (Adamo, Buruiana, Schertzer, & Boylan, 1999; Fischer, Arens, & Miller, 1998; Maltezos, Glickman, Ezzo, & He, 2006; Montellano, Schwartz, & Beeson, 2006; Scheere, Steiman, & Cohen, 2004; Torabinejad, Falah Rastegar, Kettering, &

Pitt Ford, 1995; Tselnik, Baumgartner, & Marshall, 2004), fluid filtration (Bates, Carnes, & del Rio, 1996; De Bruyne, De Bruyne, Rosiers, & De Moor, 2005; Fogel & Peikoff, 2001; Lamb, Loushine, Weller, Kimbrough, & Pashley, 2003; Wu, Kontakiotis, & Wesselink, 1998; Yatsushiro, Baumgartner, & Tinkle, 1998) , human saliva penetration (Al-Hezaimi, Naghshbandi, Oglesby, Simon, & Rotstein, 2005), and dye leakage (Andelin, Browning, Hsu, Roland, & Torabinejad, 2002; Aqrabawi, 2000; Chng, Islam, & Yap, 2005; Roy, Heansonne, & Gerrets, 2001; Stefopoulos, Tsatsas, Kerezoudis, & Eliades, 2008; Torabinejad, Higa, McKendry, & Pitt Ford, 1993; Torabinejad, Watson, & Pitt Ford, 1993; Valois & Costa, 2004) studies have attempted to directly predict the relationship of sealing capacity in retrograde materials to the *in vivo* healing outcomes. In contrast, marginal adaptation is an indirect method for evaluating the apical seal (Stabholz, Shani, Friedman, & Abed, 1985) and studies have aimed to quantify the dimensional interface between the root-end filling material and canal dentin by means of scanning electron microscopy (SEM) (Gondim et al., 2003; Shokouhinejad, Nekoofar, Ashoftehyazdi, Zahraee, & Khoshkhounejad, 2014; Stabholz et al., 1985; Torabinejad, Smith, Kettering, & Pitt Ford, 1995; Tran, He, Glickman, & Woodmansey, 2016; Xavier, Weismann, de Oliveira, Demarco, & Pozza, 2005), confocal laser scanning microscopy (CLSM) (Ravichandra et al., 2014), and micro-computed tomography (μCT) (Al Fouzan et al., 2015; Basturk, Nekoofar, Gunday, & Dummer, 2014).

The dimensional stability of root end filling materials during setting under *in vitro* conditions can vary between the manufacturer's results and the literature, with respect to how the samples were prepared and tested. The physical properties of calcium-silicate based materials should comply with the ISO 6876:2001 and ANSI/ADA No. 57:2000 standards for testing of endodontic sealers. In compliance to both standards, the mean linear shrinkage and expansion of root canal sealers should be not exceed 1% and 0.1% after 30 days, respectively (ANSI/ADA No. 57, 2000; ISO 6876, 2001). Following the recommended technique for sample preparations, materials are

compacted into three stainless-steel molds (diameter: 6 mm, height: 12 mm) and then positioned between glass plates (ANSI/ADA No. 57, 2000; ISO 6876, 2001). After five minutes, the samples are placed inside an incubator (37°C and 95% relative humidity) for the duration of three times the material's final setting time (ANSI/ADA No. 57, 2000; ISO 6876, 2001). The materials are removed from the molds and the thickness, initial length, is measured three times using an instrument, like a digital caliper, with a reported accuracy of ± 1 μm recorded to the nearest 10 μm (ANSI/ADA No. 57, 2000; ISO 6876, 2001). The three measurements are used to determine the mean initial length (L_i), which is compared to the mean final length (L_f) after being stored in distilled water for 30 days (ANSI/ADA No. 57, 2000; ISO 6876, 2001). The mean linear dimensional change (D), or strain, is calculated using the formula:

$$D\ (\%) = ((L_f - L_i)/ L_i) \times 100$$

In compliance to the aforementioned testing standards, Chng et al. (2005) and Islam et al. (2006) both investigated the hydroscopic linear expansion of W-MTA and G-MTA after 30 days and found identical results, 0.30 ± 0.01% and 0.28 ± 0.09% respectively. One of the limitations with using a restricted metal mold is detection in the horizontal direction, and the measurements only reflect the displacement in the vertical direction. Dimensional change is not an isotropic event and this understanding has lead to the experimentation of testing measurement techniques and methods.

Measuring instruments can be categorized as either a contact or noncontact devices. Another limitation in the two previously mentioned studies was the use of a caliper, which is a type of contact instrument that may not be sensitive enough to detect minor changes (ANSI/ADA No. 57, 2000; ISO 6876, 2001; Orstavik, Nordahl, & Tibballs, 2001). Like the caliper, the LVDT is also a contact instrument and can be used to measure vertical displacement in the presence of a restrained mold. In contrast to the caliper, the LVDT's contact probe is able to record a larger range, ± 4 mm, and the instrument's sensitivity is able to detect minor changes, with studies

reporting accuracy ranging from ± 0.02 µm (Storm, Eichmiller, Tordik, & Goodell, 2008), ± 0.5 µm (Gandolfi et al., 2009) and ± 2 µm (Orstavik et al., 2001). The LVDT can be programmed to record data at various time intervals and this programming has been used to investigate the hygroscopic linear expansion of endodontic materials during setting (Camilleri & Mallia, 2011; Gandolfi et al., 2009; Storm et al., 2008). Storm et al. (2008) measured the restricted dimensional change in W-MTA, G-MTA and Portland cement using LVDT and found hydroscopic expansions after submerging in water for 300 min to be 0.04 ± 0.01%, 0.47 ± 0.09%, and 0.24 ± 0.05% respectively (Figure 3A). Researchers have also combined two LVDTs to analyze the two-dimensional displacement of dental restorative materials (Kanchanavasita, Pearson, & Anstice, 1995). Experimental arrangements for LVDT used for testing endodontic materials are

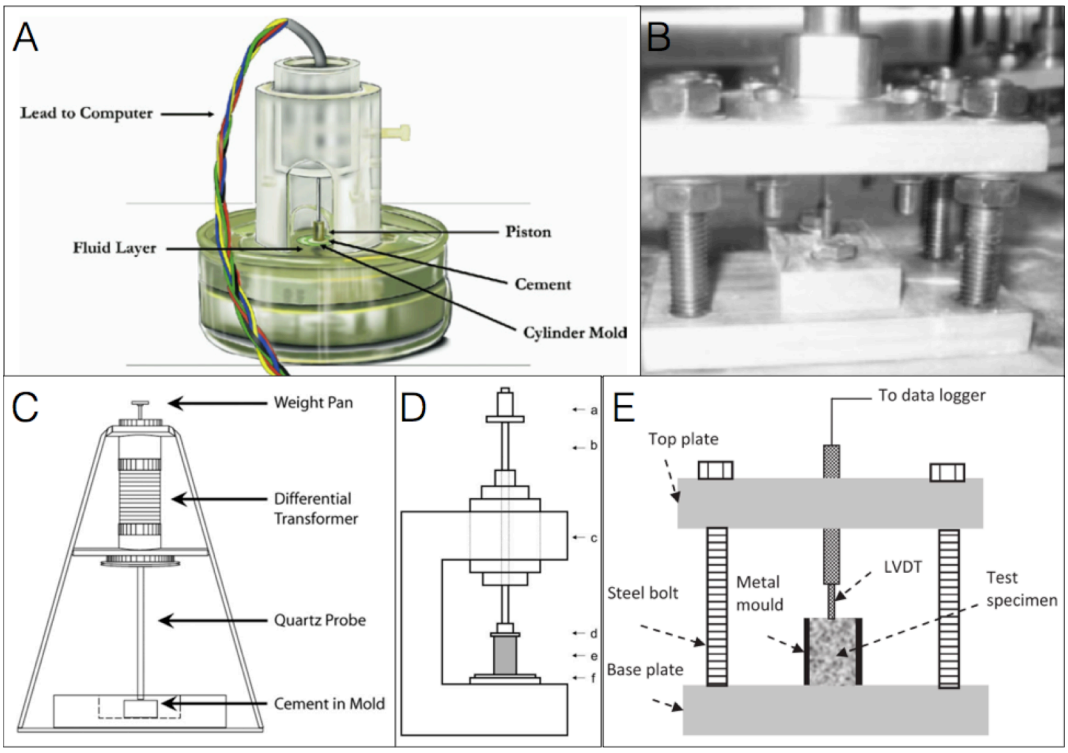

Figure 3: Experimental arrangements for LVDT used for testing endodontic materials. Photographs courtesy of (A) Storm *et al.* (2008), (B) Camilleri (2011), (C) Gandolfi *et al.* (2009) (D) Orstavik *et al.* (2001), and (E) Camilleri and Mallia (2011)

shown in Figure 3.

Contact devices, like the caliper and LVDT, are invasive in nature because they require measurements to be made, locally, on a single-point of the material's surface area. Optical methods for measuring strain have been established to address these aforementioned limitations and is a non-invasive technique that tracks deformation change, regionally, on multiple-points of the material's entire surface without requiring contact (Zhang & Arola, 2004). Image-based strain measurements have been used in previous studies to track distortion of dental materials during polymerization shrinkage (Lau, Li, Heo, & Fok, 2015; Li, Fok, Satterthwaite, & Watts, 2009; Miletic et al., 2011). DIC is an imaging recognition technique that can calculate both strain and displacement by optically tracking high contrast markers on the surface of a material. A typical arrangement for DIC is illustrated in Figure 7. Digital analysis of the initial images, before deformation, can be compared to successive images, after deformation, by digitally tracing the movement of surface reference points or "speckles" (Zhang & Arola, 2004). The precision of this measurement technique is influenced by the object's contrast and light intensities, which produces a unique gray-scale distribution (Zhang & Arola, 2004). For optimal contrast on the material's surface, the surface must be prepared. Lighter material specimens can be sprayed with a coat with black charcoal dots, whereas darker specimens are either sprayed with white dots or painted with a white background and then coated with black dots. One charge-coupled device (CCD) camera is capable of determining the two-dimensional strain by calculating the precise strain magnitude and distribution coordinates using an image-mapping gradient, with a reported detection threshold of 0.1% (Lau et al., 2015) and accuracy up to ± 0.01 pixels (Zhang & Arola, 2004). Two CCDs can be used for three-dimensional strain analysis and has been applied in dentistry (Miletic et al., 2011) and medicine (Luyckx et al., 2014).

SPECIFIC AIMS

The aim of this *in vitro* study was to evaluate the unrestricted dimensional change in the horizontal direction of ProRoot White Mineral Trioxide Aggregate, Endosequence Root Repair Material-Fast Set Putty and Biodentine in the horizontal axis during setting using the DIC technique.

NULL HYPOTHESIS

The null hypothesis states there are no significant differences in the dimensional change of three commercially available root-end filling materials.

MATERIALS AND METHODS

PILOT STUDIES

Utilizing the study design of Zedler (2016), the mean linear dimensional changes of W-MTA, ERRM-FS, and Biodentine using DIC may have been restricted by the use of a cylindrical plastic Teflon ring (Figure 4C). Therefore, designing a flexible mold to allow unrestricted expansion, in the horizontal dimensions, required the use of a flexible material. In the first pilot study, a donut ring was fabricated from an endodontic sponge using two tissue biopsy punches (internal diameter of 4mm) and placed inside a copper cylindrical ring (diameter of 8mm, height of 4mm) (Figure 4A). In this pilot study, the captured sample images (n=15) showed the presence

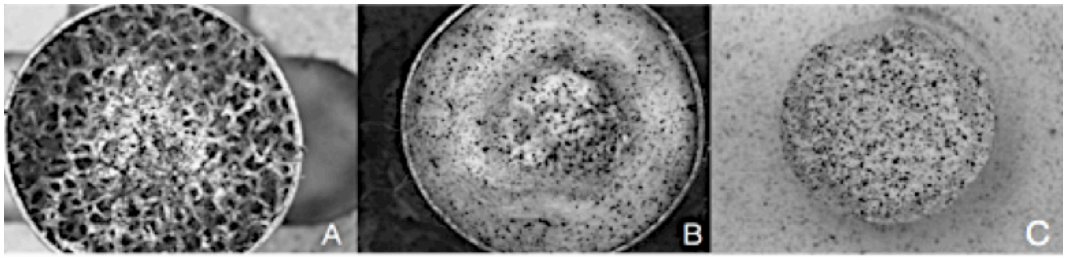

Figure 4: Pilot study molds of ERRM-FS using (A) endodontic sponge material and (B) a cotton roll material compared to restricted Teflon ring (C, photograph courtesy of (Zedler, 2016))

of the root-end filling materials infiltrating through the porosities of the dental sponge material (Figure 4A). In order to address this observation and account for the false expansion, the second pilot study replaced this material with a fibrous cotton roll, of similar dimensions (n=9) (Figure 4B). Hydration of the materials during setting was also addressed in the pilot studies. In the previous study by Zelder (2016), hydration was achieved by placing a moistened #4 cotton pellet over the material between images and by fabricating a incubator using a plastic container enclosed with two saturated cotton rolls at room temperature at 80% humidity (Zedler, 2016). The author noted that refreshing the #4 cotton pellet with saline between images could have caused distortion due to the direct oversaturation of surface reference points (Zedler, 2016). Therefore,

the first and second pilot studies tried to address oversaturation by adding100 uL/hr aliquots of saline onto the flexible material surface with a 100 uL pipette. The volume of saline added was chosen to reflect the mean daily volume of gingival crevicular fluid secreted in a healthy mouth, 0.5-2.4 mL (Challacombe, Russell, Hawkes, Bergmeier, & Lehner, 1978). In the second pilot study, the cotton roll material was uniformly saturated between images whereas, in the first pilot study, the dental sponge material showed the presence of localized droplets between images. Any presence of a glossy image from over-saturation became difficult for the software to analyze and was omitted in the data analysis. Additionally, stabilizing the samples during their setting time intervals was necessary because movement of the camera or sample would distort the analyzed data. In the first and second pilot studies, the incubator was similar to the previous study design and required delicate removal to capture images and hydrate samples during their respected setting intervals. The presence of minor movements was observed in all pilot studies. In absence of a well-controlled hydration method, another disadvantage in the mold design was the difficulty to standardize the volume of material compacted into a flexible mold, volume of 50.27mm^3 (Figure 4). An additionally inconsistency with using a flexible mold was maintaining a uniform

Figure 5: A plaster of Paris split mold with a volume of 19.63 mm^3 (internal diameter: 2.5 mm; height: 4 mm)

flat surface during image analysis, as the material showed unrestricted movement into porosities or voids on the surface which affected the camera's focus in the first and second studies respectively.

The mentioned limitations of standardization and image stabilization from the previous two pilot studies were addressed in a third pilot study (n=6). In this study, a split mold was fabricated using low-expansion plaster of Paris (WhipMix, Louisville, KY) and polished with 1200 grit sand paper (Figure 5). The internal diameter and height of the split mold was 2.5 mm x 4 mm, respectfully, with a volume of 19.63 mm^3 (Figure 5). In the pilot studies, the internal humidity may be disrupted by the continued removal of the incubator in order to capture images during the setting time intervals. Likewise, an incubator box with a clear lid was fabricated to capture images throughout the experimental duration (Figure 7). However, in the presence of a relative high humidity and body temperature, condensation inside the incubator affected the quality of images collected during the setting intervals and lid removal would be inevitable. Thus, all interval images captured before the final set were eliminated, and the camera and incubator were secured to prevent movement distortion of the final image (Figure 7). Images captured in the third pilot and present study were initial (0 minutes) and final set; W-MTA (240 minutes), ERRM-FS (240 minutes), and Biodentine (60 minutes).

SAMPLE PREPARATION

Three commercially available root-end filling materials were used in the present study: W-MTA (Lot 129580), ERRM-FS Putty (Lot 1602FSPS), and Biodentine (Lot B19843) (Figure 6). Based on pilot studies 1 and 2, a sample size of 10 per experimental group was used, yielding a 82% power to detect a 1.5 standard deviation from the mean. Three Filtek™-LS composite (Shade A1, 3M ESPE, St. Paul, MN; Lot N730352) samples and three Cavit™ G (3M ESPE St. Paul, MN; Lot 626297) samples were used as the positive controls for shrinkage and expansion,

Figure 6: Experimental root-end filling materials groups; W-MTA, ERRM-FS, and Biodentine (photograph courtesy of (Zedler, 2016))

respectively. Manufacturer's instructions for curing the composite required 40 seconds using a LED light, with a 500 mW/cm^2 light intensity (MSDS, 2008). The final images for composite samples was immediately after polymerization, whereas the final images for Cavit samples were experimentally set at 75 minutes based on the findings by Ono and Matsumoto (1992) (Ono & Matsumoto, 1992). Two empty samples were used as the negative control to account for background noise during image analysis. W-MTA and Biodentine samples were prepared according to the manufacturer's instructions, whereas the ERRM-FS samples were already prepared in a premixed syringe. W-MTA powder (1 gram) was mixed with the supplied aliquot of liquid (0.35 grams) on a glass slab using a metal spatula (MSDS, 2002). Biodentine was prepared by adding five aliquots of liquid and then triturated in an amalgamator for 30 seconds at a setting of 4000±200 rpms (MSDS, 2010).

The split molds were fabricated with plaster of Paris (Lot 010051701) and incubated, at 37°C and 95% relative humidity, for 24 hours prior to being testing in accordance with ISO 6876:2001 and ANSI/ADA No. 57:2000 standards for testing the setting time of endodontic sealers, with the exception of mold dimensions. The experimental materials were compacted into the molds using a carrier (MAP system, Produitis Dentaires, Vevey, Switzerland) and condensed with a size #1 Buchanan Hand Plugger (Sybron Dental Specialities Inc, Orange, GA) until flush by one endodontic resident operator. Samples were then placed inside the incubator with the camera focused on the center of the materials surface and the surface was sprayed with an even layer of charcoal carbon powder.

Each sample was imaged twice using a charged-coupled device (CCD) camera (Point Gray Grasshopper GRAS- 20S4C-C). The first image was acquired immediately after initial mix and used as the reference image for comparison against the second image, after final set. Based on pilot studies, the experimental setting times for W-MTA and ERRM-FS samples was designated at 240 minutes and Biodentine at 60 minutes. The samples were maintained in an incubator, with a relative high humidity (>95%) in 37°C, throughout the duration of experiment. The CCD camera and incubator were both fixated to the base using stabilizing screws in order to prevent additional movement during lid removal. The CCD camera captured each image at a frequency of 1.875 Hz and had a documented spatial resolution of 1392 x 1051 pixels. The pixel intensities were mapped using 256-color palette with a maximum gray-scale intensity of 4095. A scaling factor of 410.2 pixel/mm and pixel size of 0.0067 mm was calibrated from a stock image, measuring 0.16 μm in diameter x 0.60 μm apart. The imaging set up, including the sample in the

split mold, the CCD camera, the incubator, and the mounted based, is illustrated in Figure 7.

STATISTICAL ANALYSIS

Strain analysis and the mean linear displacement were analyzed using a proprietary software (StrainMaster, Davis 7.0 LaVision GmbH, Germany). The mean linear dimensional changes was calculated from the displacement of surface landmarks in the x-axis, Exx, and y-axis, Eyy, in a field of view of 12.56 mm^2. The mean magnitude of two-dimensional change, 2D%Strain, was calculated from the displacement in the xy-plane. Descriptive statistics were used to summarize the pixel intensity mapping for overall strain and the vector displacement absolute velocity. Strain analysis and displacement was carried out using the analysis of variance (ANOVA) and Turkey's post hoc test ($p < 0.05$) with a software system (SAS V09.3 for

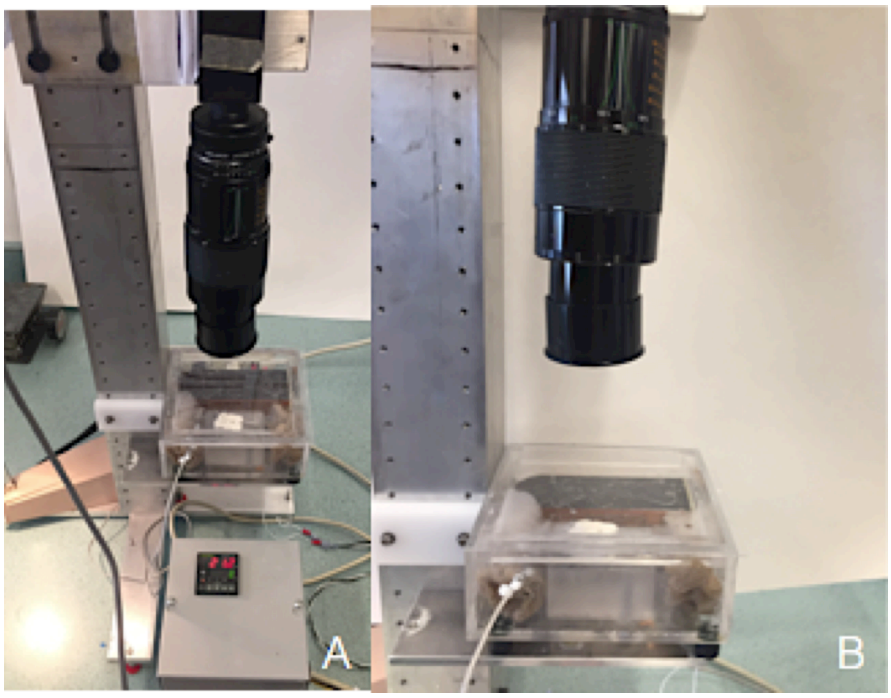

Figure 7: The experimental test set up included fixation of the CCD camera and incubator to the base, and the temperature and humidity sensors (A) connected to the incubator. The camera was positioned over the center of the split mold (B).

Windows).

RESULTS

DISPLACEMENT ANALYSIS

The mean, standard deviation, minimum and maximum strain values in the x-axis, Exx, y-axis, Eyy and two-dimensions, 2D%Strain, were analyzed for each of the experimental groups (Table 4). A negative number indicates compression, or shrinkage, and a positive number indicates tension, or expansion. The mean percentages of Exx, Eyy, and 2D%Strain were compared between the Biodentine, ERRM-FS, and W-MTA groups with a one-way ANOVA. The means were statistically significantly different, $p < 0.0001$. In pairwise comparisons, the mean 2D%Strain for ERRM-FS was larger compared to Biodentine and MTA, $p=0.0001$ and $p=0.0009$ respectively. P-values for pairwise comparisons were adjusted for multiple comparisons using the Turkey's post hoc test.

Group	N Obs	Variable	N	N Miss	Mean	Std Dev	Med	Min	Max
Biodentine	10	Exx	10	0	-0.02	0.22	-0.03	-0.31	0.33
		Eyy	10	0	-0.02	0.14	-0.02	-0.2	0.2
		Strain %	10	0	-0.01	0.21	-0.01	-0.3	0.27
ERRM-FS	10	Exx	10	0	1.53	1.36	0.86	0.38	4.1
		Eyy	10	0	0.32	0.26	0.27	-0.03	0.76
		Strain %	10	0	1.86	1.34	1.34	0.48	4.24
W-MTA	10	Exx	10	0	0.22	0.42	0.09	-0.15	1.17
		Eyy	10	0	0.07	0.22	0.11	-0.36	0.36
		Strain %	10	0	0.29	0.57	0.16	-0.39	1.37
Cavit	3	Exx	3	0	2.81	1.34	2.87	1.44	4.12
		Eyy	3	0	1.39	0.18	1.45	1.18	1.53
		Strain %	3	0	4.2	1.39	4.05	2.89	5.65
Composite	3	Exx	3	0	-0.7	0.04	-0.72	-0.73	-0.66
		Eyy	3	0	-0.44	0.04	-0.44	-0.48	-0.39
		Strain %	3	0	-1.14	0.05	-1.13	-1.2	-1.11
Empty	2	Exx	2	0	-0.29	0.03	-0.29	-0.31	-0.27
		Eyy	2	0	0.34	0.07	0.34	0.28	0.39
		Strain %	2	0	0.04	0.04	0.04	0.01	0.07

Table 4: Analysis of variance for mean strain in the experimental groups

Crack	Group	N Obs	Variable	N	N Miss	Mean	Std Dev	Median	Min	Max
0	Biodentine	10	Exx	10	0	-0.02	0.22	-0.03	-	0.33
			Eyy	10	0	-0.02	0.14	-0.02	-0.2	0.2
			Strain %	10	0	-0.01	0.21	-0.01	-0.3	0.27
	ERRM-FS	4	Exx	4	0	0.58	0.1	0.54	0.51	0.74
			Eyy	4	0	0.13	0.13	0.13	-	0.29
			Strain %	4	0	0.71	0.19	0.74	0.48	0.88
	W-MTA	8	Exx	8	0	0.05	0.19	-0.01	-	0.33
			Eyy	8	0	0.02	0.21	0.06	-	0.33
			Strain %	8	0	0.06	0.36	0.07	-	0.66
	Cavit	1	Exx	1	0	1.44	-	1.44	1.44	1.44
			Eyy	1	0	1.45	-	1.45	1.45	1.45
			Strain %	1	0	2.89	-	2.89	2.89	2.9
	Composite	3	Exx	3	0	-0.7	0.04	-0.72	-	-
			Eyy	3	0	-0.44	0.04	-0.44	-	-
			Strain %	3	0	-1.14	0.05	-1.13	-1.2	-
	Empty	2	Exx	2	0	-0.29	0.03	-0.29	-	-
			Eyy	2	0	0.34	0.07	0.34	0.28	0.39
			Strain %	2	0	0.04	0.04	0.04	0.01	0.07
Crack	**Group**	**N Obs**	**Variable**	**N**	**N Miss**	**Mean**	**Std Dev**	**Median**	**Min**	**Max**
1	ERRM-FS	6	Exx	6	0	2.17	1.45	2.01	0.38	4.1
			Eyy	6	0	0.45	0.24	0.44	0.14	0.76
			Strain %	6	0	2.62	1.22	2.52	1.14	4.24
	W-MTA	2	Exx	2	0	0.9	0.39	0.9	0.62	1.17
			Eyy	2	0	0.28	0.12	0.28	0.2	0.36
			Strain %	2	0	1.18	0.27	1.18	0.98	1.37
	Cavit	2	Exx	2	0	3.5	0.89	3.5	2.87	4.12
			Eyy	2	0	1.36	0.25	1.36	1.18	1.53
			Strain %	2	0	4.85	1.13	4.85	4.05	5.65

Table 5: Two-way analysis of variance on mean strain in the experimental groups and the

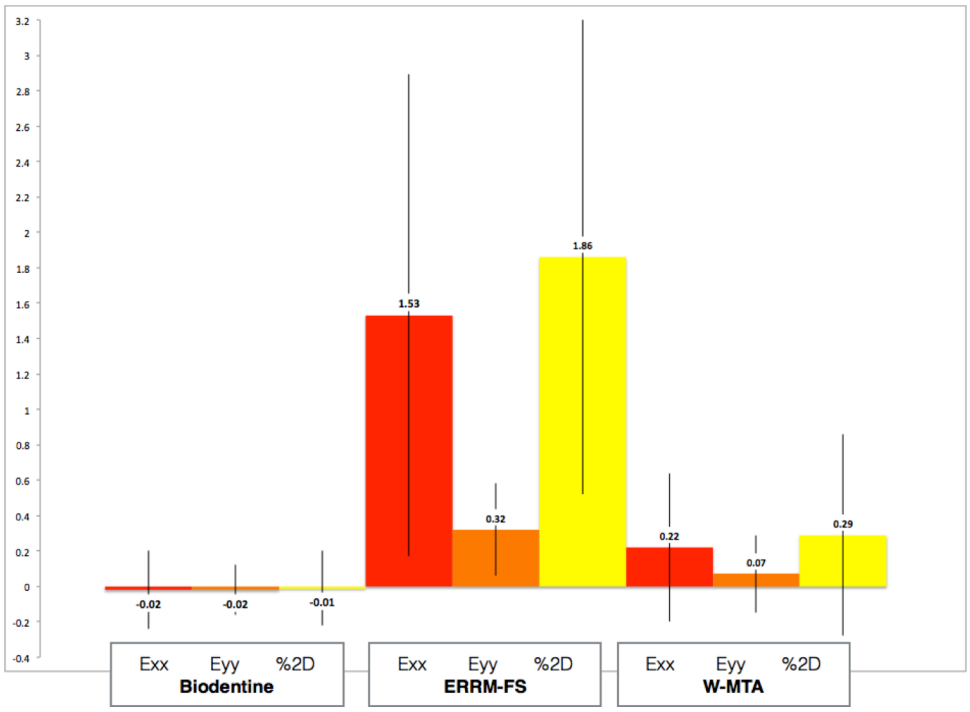

Table 6: Analysis of variance for the mean Exx, Eyy, and 2D%Strain for Biodentine, ERRM-FS, and W-MTA (SD shown in error bars)

INTENSITY MAPPING

The image displacement scale was calibrated using a reference image, and represented in both a metric (mm) and a raw data location (pixels). In the present study, the image-scaling factor was 410.2 pixel/mm and the average field of view was 4.91 mm^2, with a material diameter of 2.5 mm. For 2D%Strain of Biodentine, shrinkage was present in half of the samples (n=5) and always observed when both the Exx and Eyy values were negative (n=2, Samples 2 and 10). Similar to composite, there was a trend for shrinkage to occur with greater compression in the Exx direction (Samples 6, 7, and 10) compared to Eyy direction (Samples 2 and 4), but this consistent finding was an inverse feature for W-MTA (Table 5). For 2D%Strain of W-MTA, shrinkage was present in approximately a third of the group (n=3) and always observed when both the Exx and Eyy values were negative (n=3, Samples 1, 5 and 8). A typical shrinkage or negative 2D%Strain

displacement of materials contained some heterogeneous features, as shown in Figure 10. In the positive control for shrinkage, Filtek composite group (n=3), compression in the Exx direction was greater than the Eyy for all samples, and both values were always negative (Table 7). Compared against the experimental groups that displayed shrinkage (n=8), no trend between greater compression values in the Exx (n=4) or Eyy (n=4) could be determined, with the

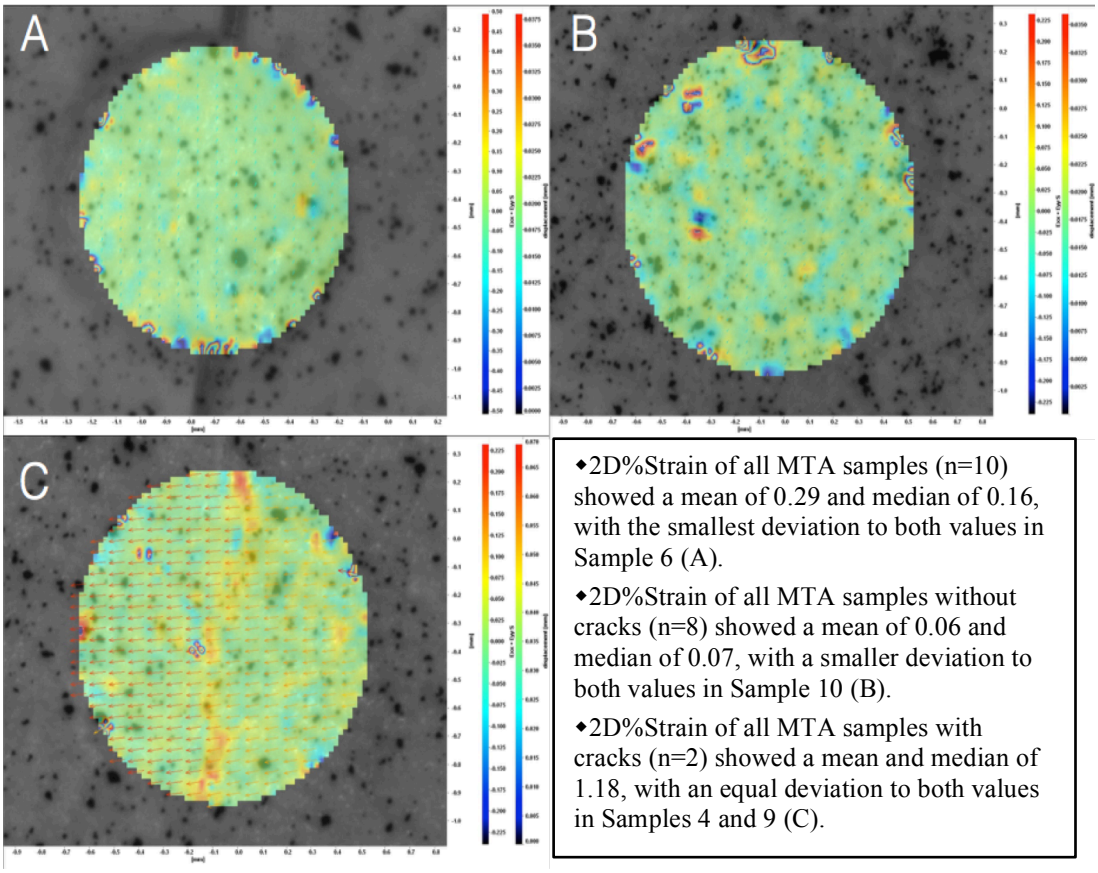

Figure 8: Intensity mapping and vector display of W-MTA samples

exception that shrinkage always occurred when both values were negative (n=5).

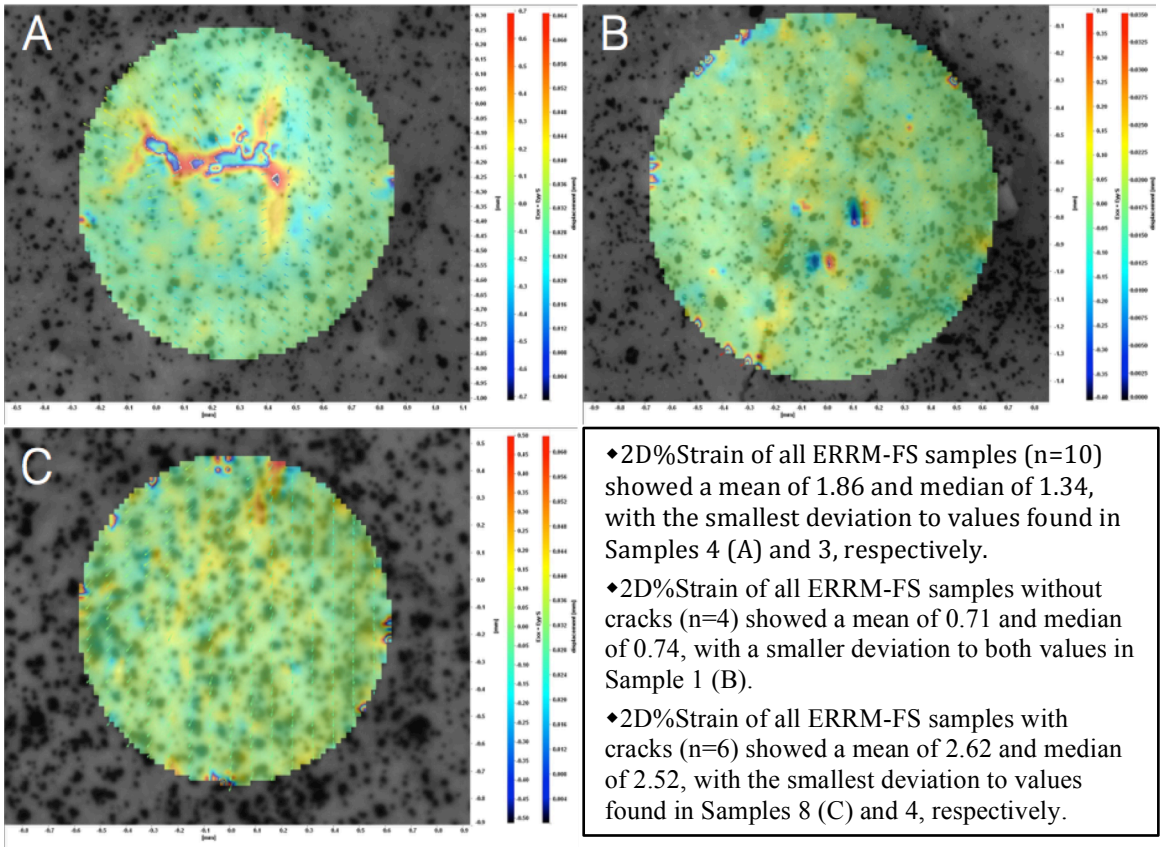

- 2D%Strain of all ERRM-FS samples (n=10) showed a mean of 1.86 and median of 1.34, with the smallest deviation to values found in Samples 4 (A) and 3, respectively.
- 2D%Strain of all ERRM-FS samples without cracks (n=4) showed a mean of 0.71 and median of 0.74, with a smaller deviation to both values in Sample 1 (B).
- 2D%Strain of all ERRM-FS samples with cracks (n=6) showed a mean of 2.62 and median of 2.52, with the smallest deviation to values found in Samples 8 (C) and 4, respectively.

Figure 9: Intensity mapping and vector display of ERRM-FS samples

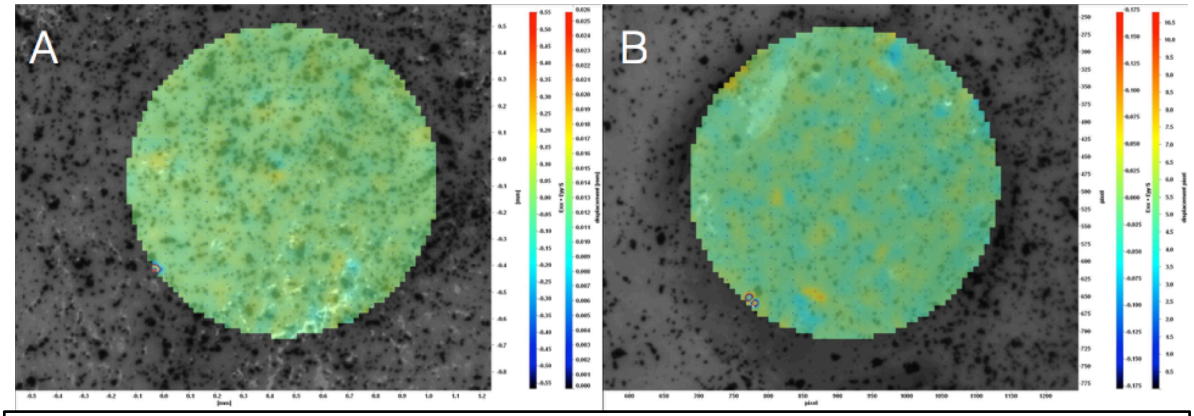

- 2D%Strain of all Biodentine samples (n=10) showed a mean and median of -0.01, with the smallest deviation to both values found in Sample 6 (A).
- *Postive Control (Shrinkage):* 2D%Strain of all Composite samples (n=3) showed a mean of -1.14 and median of -1.13, with a smaller deviation to both values in Sample 1 (B).

Figure 10: Intensity mapping and vector display of Biodentine sample and positive control

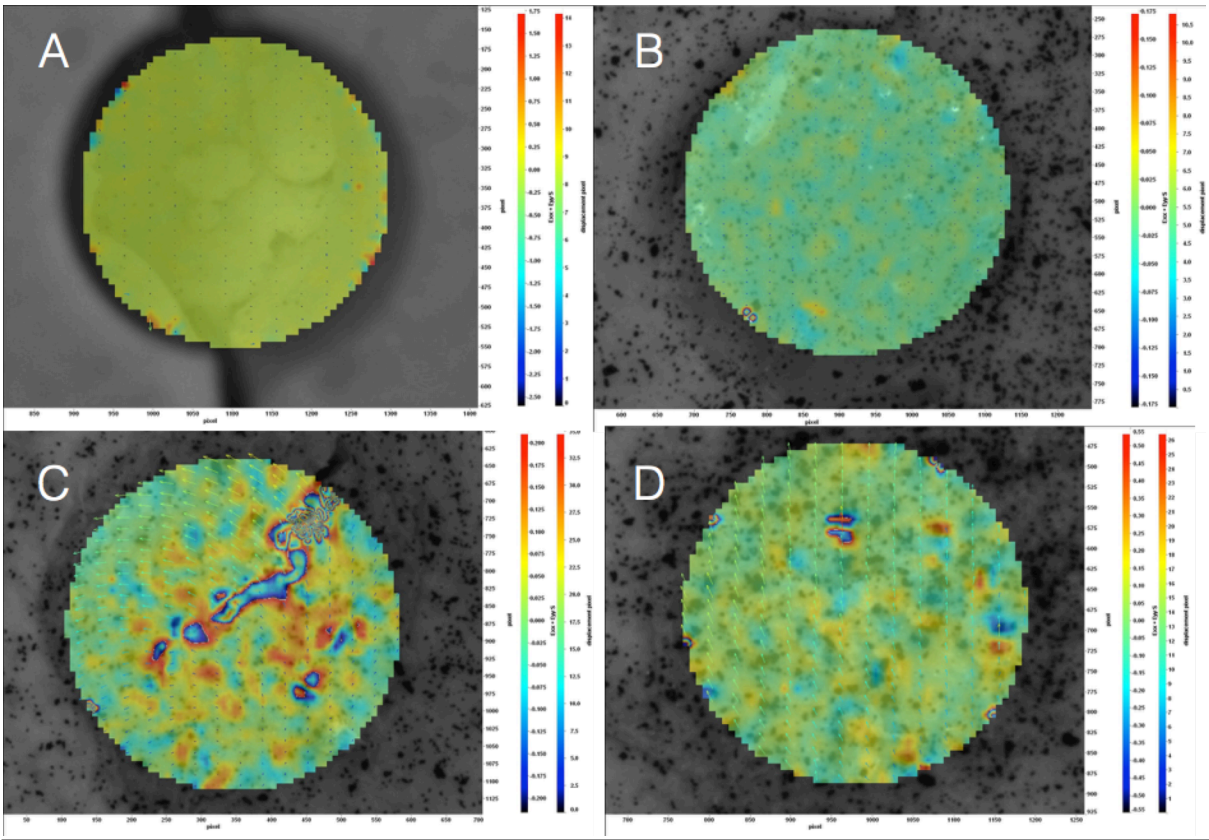

- *Negative control (Background noise):* 2D%Strain of all Empty samples (n=2) showed a mean and median of 0.04 with an equal deviation to both values in Samples 1 and 2 (A).
- *Postive Control (Shrinkage):* 2D%Strain of all Composite samples (n=3) showed a mean of -1.14 and median of -1.13, with a smaller deviation to both values in Sample 1 (B).
- *Positive Control (Expansion):* 2D%Strain of all Cavit samples (n=3) showed a mean of 4.20 and median of 4.05, with the smallest deviation to both values in Sample 3 (C). Similar deviation of Sample 3 was found for the 2D%Strain of all Cavit samples with cracks (n=2), mean and median of 4.85. 2D%Strain of all Cavit samples without cracks (Sample 1, D) showed a mean and median of 1.44.

Figure 11: Intensity mapping and vector display of all control samples

EFFECT OF CRACKS

Cracks were observed after 240 minutes for W-MTA (n=2) and ERRM-FS (n=6) samples. To investigate the effect of the cracks, a two-way ANOVA was run. The group effect remained significant (p=0.0096) and effect of the cracks was significant (p<0.0001). The mean 2D%Strain for cracked samples was 1.88 versus 0.29 for non-cracked samples. A one-way ANOVA was run again, removing the cracked samples. Results were similar. The means were statistically significantly different, p=0.0008. In pairwise comparisons, the mean 2D%Strain for ERRM-FS was larger compared to Biodentine and W-MTA, p=0.0007 and p=0.0029 respectively.

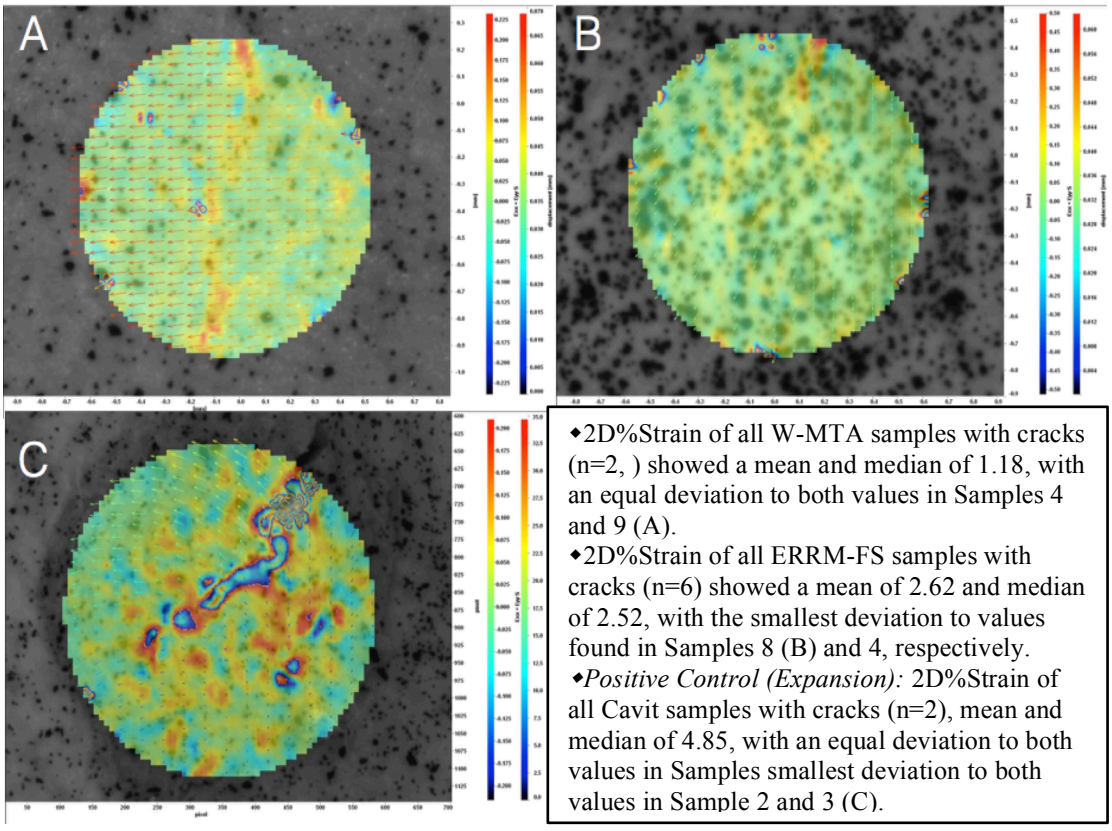

Figure 12: Intensity mapping and vector display of all samples with cracks

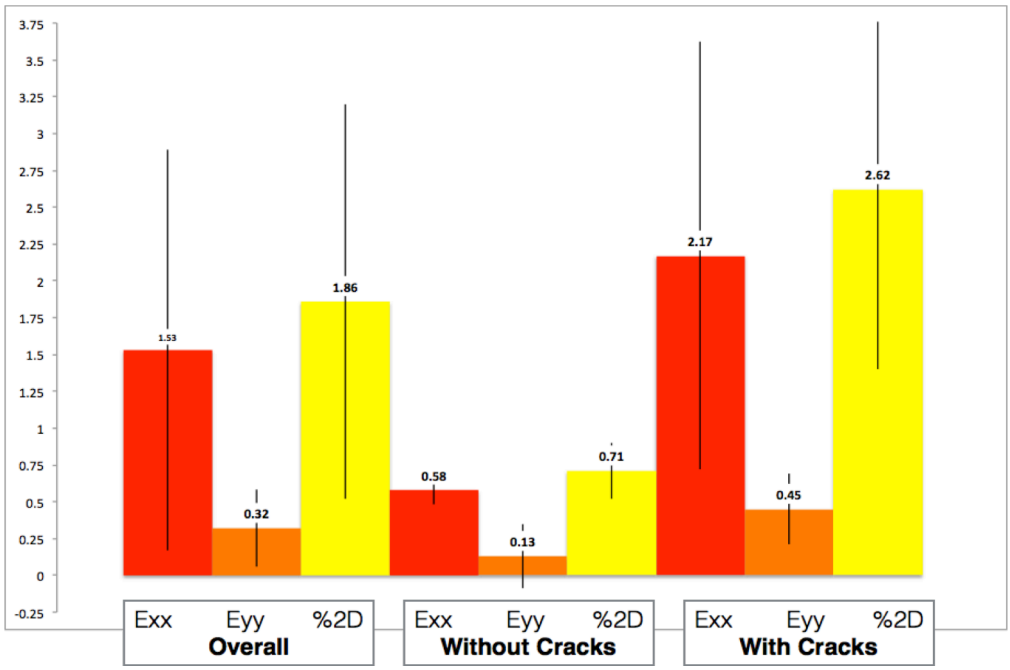

Table 7: Analysis of variance for the mean Exx, Eyy, and %2DStrain for overall ERRM-FS, ERRM-FS without cracks, ERRM-FS with cracks (SD shown in error bars)

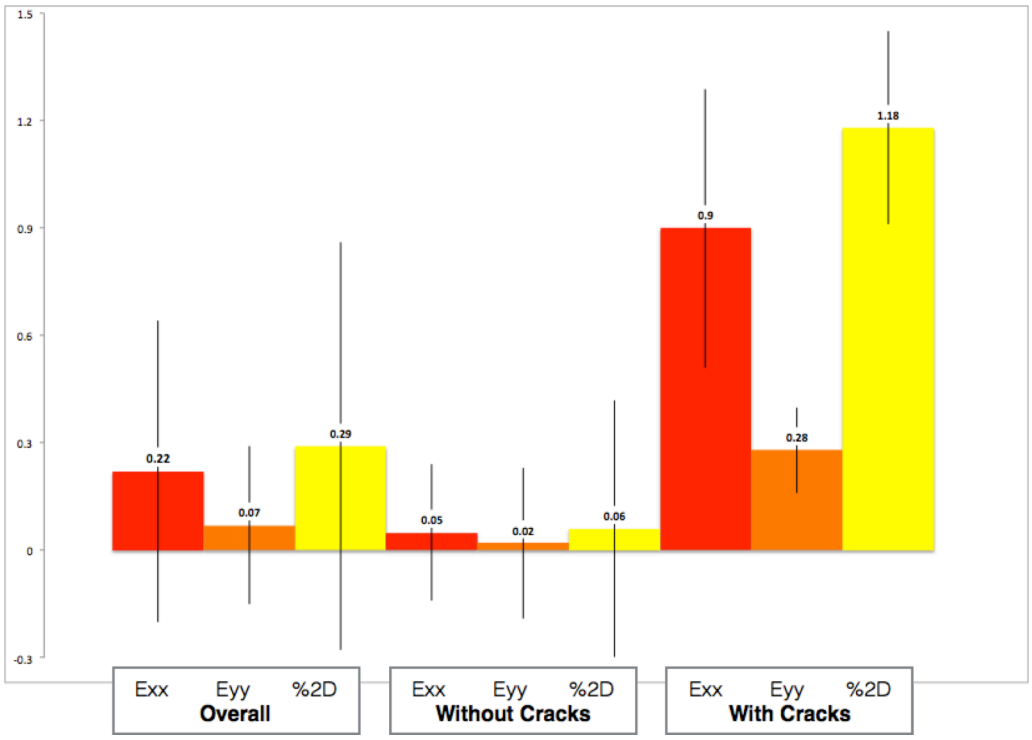

Table 8: Analysis of variance for the mean Exx, Eyy, and %2DStrain for overall W-MTA, W-MTA without cracks, W-MTA with cracks (SD shown in error bars)

DISCUSSION

Calcium-silicate based materials undergo two hydration reactions during setting, and the by-products that are formed contribute to the material's bioactivity, a characteristic responsible for its preferred use as a root-end filling material in modern apical surgery. Many *in vitro* studies have focused on the physical properties of these materials and an indirect method for evaluating a material's sealing capacity includes the dimensional stability during setting. In the present study, three experimental groups were selected based on their similar chemical composition, specifically tri- and dicalcium silicates, and the unrestricted horizontal displacement was measured using DIC. Within the limitations of this study, two-dimensional strain measured by means of DIC is validated for W-MTA and Biodentine samples, but inconclusive for ERRM-FS.

The background noise present in the negative control groups had a mean linear expansion of 0.04 ± 0.04%, with a maximum expansion reaching 0.07% (Table 4). Given the small expansion and standard deviation of the empty samples, the accuracy for measuring two-dimensional strain in the horizontal direction using DIC should not be effected. Cavit™ G is premixed provision material that is primarily composed of zinc oxide, calcium sulfate, and polyvinyl acetate resins and requires hydration in order to set (Widerman, Eames, & Serene, 1971). In a study by Widerman et al. (1971), the authors mixed Cavit with 10:1 proportions of water and after 10 days immersion in distilled water, the hygroscopic liner expansion was found to be 14.20 ± 0.09 %, absorbing approximately 18% of its weight in water after 3 hours. In the present study, Cavit was dispensed following manufacturer's instructions and the mean linear expansion of Cavit (n=3) was found to be 4.20 ± 1.39% after 75 minutes (Table 4). Intensity mapping of two Cavit samples showed the presence of cracking after 75 minutes, with a vector displacement of approximately 201 μm radiating from the center of the crack (Figure 12 C). Widerman et al. (1971) reported similar displacement values, where the authors disclosed a 0.15 ± 0.05 mm discrepancy in crown heights due to hydroscopic expansion. In the present study, Cavit was used as a positive control

for expansion and composite used for shrinkage. The mean linear shrinkage immediately after polymerization for the composite group was -1.14 ± 0.05%, with a maximum shrinkage of -1.20 % (Table 4). These results were comparable to a DIC study by Lau et al. (2015), where the authors reported a -1.19% net shrinkage of Filtek™-LS after polymerization.

The mean linear expansion between the initial and final setting time, 240 minutes, for W-MTA was 0.29 ± 0.57%, with a maximum expansion of 1.37 % (Table 4). In the present study, the mean linear expansion was similar to studies by Chng et al. (2005), Islam et al. (2006), and Shahi et al. (2015), where the authors reported slight expansion, 0.30%, of W-MTA after 30 days of immersion in distilled water in compliance to ISO 6876:2001 methods. Under compliance to these testing methods, the initial length is measured after the material has been allowed to set three times longer than the measured setting time (ANSI/ADA No. 57, 2000; ISO 6876, 2001). In all of the mentioned studies, the authors did not report the duration before initial measurement. Chng et al. (2005) and Islam et al. (2006) reported the final setting time of W-MTA to be 140 minutes, whereas Shahi et al. (2015) reported 35 minutes. Therefore one can postulate the initial measurements were taken approximately 420 and 105 minutes later, respectively. Although these aforementioned studies had similar expansions to the present study, variations in the experimental design duration may be a contributing factor to the reported dimensional changes in the literature. In a study by Gandolfi et al. (2009), W-MTA showed 0.77 ± 0.27% net expansion after being immersed in distilled water for 180 minutes, and the authors reported the initial lengths measured were after the material was allowed to set for 30 minutes at 37 °C and 50% humidity. In a study by Storm et al. (2008), the authors reported net expansion of W-MTA using LVDT for a duration of 24 hours and the samples were allowed to harden at room temperature for an undisclosed duration prior to being tested. Expansion of more than 0.6% was reported in a study by Wiltbank et al. (2007), where W-MTA samples were allowed to set for 48 hours wrapped in a moisten-gauze and stored in 37 °C and 100% humidity, and the total duration of this study was 30 days.

W-MTA showed 0.095% hydroscopic shrinkage in a LVDT study by Camilleri (2011) and the author allowed the material to cure for 24 hours in 37 °C and 100% humidity, with an experimental duration of 28 days. Camilleri and Mallia (2011) reported net shrinkage of W-MTA after 7 days in 100% humidity, where the material was allowed to set, 140 minutes, in 37 °C and 100% humidity. In a recent study by Bernardi et al. (2017), the authors kept W-MTA samples at body temperature in 95% humidity for 24 hours but did not report the dimensional change after 30 days immersed in distilled water. Net shrinkage was also reported for W-MTA in the study by Zedler (2016), where the samples were kept at 80% humidity after initial mixing and for the duration of 240 minutes. The authors reported W-MTA to have a linear shrinkage of -1.843 ± 0.614% using DIC, which is more than the recommended 1% shrinkage for endodontic sealers. In the present study, measuring the initial length immediately after mixing mimics a clinical situation.

In the current study, the volume dimensions and split-mold design using plaster of Paris proved to be more suitable than the molds recommended in the ISO 6876:2001 and ANSI/ADA No. 57:2000 standards for testing the dimensional stability of sealers. Compared to the recommended stainless-steel molds (diameter: 6 mm, height: 12 mm), the present study complied with the ISO 6876:2001 and ANSI/ADA No. 57:2000 standards for testing the setting time of sealers that require moisture during setting, with the exception of volume dimensions (diameter: 10 mm, height: 5 mm) that were modified to reflect the root-end preparation cavity (Figure 5). A variety of mold sizes and materials have been utilized in various studies. Gandolfi et al. (2009) fabricated an aluminum well (diameter: 11 mm, height: 5 mm) only open at the top, and Storm et al. (2008) and Hawley et al. (2010) both used cylindrical polyvinyl siloxane molds with various diameters to yield 0.6 g of material. Camilleri (2011) and Camilleri and Mallia (2011) both used an undisclosed metal mold (diameter: 5 mm, height: 10 mm) coated with oil (Seperol), and an undisclosed material (diameter: 3 mm, height: 6 mm) yielding 0.5 g of sample mass also reported

in the study by Wiltbank et al. (2007). Zedler (2016), Bernardi et al. (2017), and Shahi et al. (2015) all used teflon molds but with different height and depth dimensions.

The mean linear shrinkage between the initial and final setting times, 60 minutes, for Biodentine was -0.01 ± 0.21%, with a maximum shrinkage of -0.30 % (Table 4). The mean linear expansion between the initial and final setting time, 240 minutes, for ERRM-FS was 1.86 ± 1.34%, with a maximum expansion of 4.24 % (Table 4). The mean and standard deviations for overall strain for ERRM-FS in the Exx and Eyy directions were found to be 0.22 ± 0.42% and 0.07 ± 0.22%, respectively (Table 4). There were more fluctuations in the x-direction compared to the y-direction, consistent with the positive control for hydroscopic expansion, and Exx was always greater than Eyy (Table 4). In the present study, the linear expansion for ERRM-FS was similar to other reports (Zedler, 2016). However, Biodentine shrinkage was 100 times less than that reported by Zedler (2016), -1.302 ± 0.416, and this may be due to differences in relative humidity and restrained mold. The liquid component of Biodentine contains calcium chloride, which accelerates the reaction between tricalcium silicate and gypsum (Ramachundran, 1992), and polycarboxylate, which is a hydrosoluble polymer designed to reduce the water content and increase the material's flow (Table 9). As such, Biodentine has a reported manufactured setting time of 12 minutes and is faster compared to W-MTA with no accelerant (Wiltbank, Schwartz, & Schindler, 2007). Kaup et al. (2015) reported a setting time for Biodentine to be almost 86 minutes, while Grech et al. (2013) reported a 45-minute setting time. When W-MTA is mixed with 5% calcium chloride, Wiltbank et al. (2007) reported the setting time was reduced by 35 minutes and the linear expansion showed a slight decrease, but not significantly different. In a study by Kogan et al. (2006), MTA mixed with 3% and 5% calcium chloride additives showed a significant reduction in setting times, 50 and 25 minutes respectively. Wongkornchaowalit and Lertchirakarn (2011) reported a significant reduction of the setting times and increased flowability of Portland cement when mixed with polycarboxylate at concentrations of 1.8% and

2.4%. Rapid setting retrograde materials are preferred to minimize the potential for washout, which is clinically relevant when placing a retrograde material.

Shrinkage of Biodentine samples may be related to cement's porosity and particle diameter. Compared to W-MTA, Biodentine has smaller calcium-silicate powder grains compared, with reported pore diameters ranging from 0.0121 μm (Camilleri et al., 2014) to 7.510 μm (Ha et al., 2017), for Biodentine, and 19.386 μm (Ha et al., 2017) for W-MTA. Bentz and Aitcin (2008) described the hidden meaning behind the water to cement powder ratios, postulating a direct link to spacing between the particles and setting time. Smaller grain particles will hydrate more quickly than larger particles and fill in the spaces between the unhydrated particles, owing to the material's faster hydration rate (Bentz & Aitcin, 2008). However, smaller particles may generate stress during drying and result in shrinkage. Like Biodentine, ERRM-FS has a smaller particle diameter and faster setting time, however in the present study the material did not seem to be fully cured. The material was still flaky at the end of the experiment, which may have been contributed by the environmental conditions and absence of saturation. Similar findings were also observed in the study by Zedler (2016), where the author described unset ERRM-FS samples after 4 hours. Several studies have also confirmed difficulties with ERRM

Powder	W-MTA	ERRM-FS	Biodentine
	tricalcium silicate	tricalcium silicate	tricalcium silicate
	dicalcium silicate	dicalcium silicate	dicalcium silicate
	tricalcium aluminate	calcium phosphate monobasic	calcium carbonate
	calcium sulfate dihydrate	calcium sulfate anhydrate	calcium oxide
	bismuth oxide	zirconium oxide	zirconium oxide
		tantalum pentoxide	iron oxide
Liquid			
	distilled water		distilled water
			calcium chloride
			hydrosoluble polymer

Table 9: The chemical composition of W-MTA, ERRM-FS, and Biodentine

setting, where none of the ERRM samples appeared fully set at 48 hours, in dry or saturated conditions (Charland, Hartwell, Hirschberg, & Patel, 2013). In a study by Damas et al. (2011), ERRM was fully set at 168 hours in 100% humidity, but none were set at 24, 72, or 120 hours under similar conditions.

Variations of the dimensional stability reported in literature may be due to the method of mixing and varying the water to powder ratio. Compared to MTA's manual mixing, Biodentine is mixed by an amalgamator, which produces a more homogenous cement mixture, whereas ERRM-FS is dispensed in a preloaded syringe. In a study by Shahi et al. (2015), the authors investigated the dimensional stability of MTA using various mixing techniques and found similar expansion, 0.3 ± 0.09%, with the conventional technique used in the present study. In the same study, the authors mixed MTA with ultrasonic activation or an amalgamator and reported an increase in expansion of MTA, 0.4 ± 0.09% and 0.35 ± 0.01% respectively. In the present study, the specimens were compacted into the plaster of Paris mold using a plugger to simulate clinical conditions. Studies comparing the dimensional stability of retorgrade materials have used other techniques. Camilleri (2011) compacted materials into three increments, similar to the Camilleri and Mallia (2011) study, whereas Wiltbank et al. (2007), Storm et al. (2008), and Hawley et al. (2010) all used ultrasonic energy. Basturk et al. (2014) demonstrated that manual mixing of W-MTA showed higher porosities compared to mechanical vibration and ultrasonication, however Yeung et al. (2006) showed that a denser fill is achieved for manual mixing with indirect ultrasonic activation. In a study by Aminoshariae et al. (2003), the authors reported more voids in MTA with direct ultrasonic activation compared to hand condensation, and the authors also concluded that the 3:1 recommended powder to water ratio may produce more porosities. This ratio is recommended for complete hydration (Fridland & Rosado, 2003) and is consistent with the manufactured 0.35 g. water ampoule packaged in ProRoot MTA. Neekofar et al. (2009) claimed that this water amount is not consistently present in the provided ampoule, and the

authors found water differences ranging from 0.139 to 0.198 g. less than the manufacturer's claim. Hawley et al. (2010) investigated the linear expansion using LVDT with various water to powder ratios. Similar to the water powder ratio in the present study, the authors found expansion of W-MTA and G-MTA to be 0.086 ± 0.029% and 2.15 ± 0.0337%, respectively. The authors concluded no significant differences in expansion to the control, 0.35, when varying the water to powder ratios, 0.26, 0.28, and 0.30, however all samples were saturated in a physiological solution and may have contributed to their findings (Hawley, Webb, & Goodell, 2010).

The dimensional stability of retrograde materials have been investigated when immersed in physiological solutions (Camilleri, 2011; Camilleri & Mallia, 2011; Hawley et al., 2010; Storm et al., 2008), whereas others have followed the ISO recommendations by using distilled water (Bernardi et al., 2017; Chng et al., 2005; Islam, Chng, & Yap, 2006; Wiltbank et al., 2007; Zedler, 2016). Variations in dimensional changes may also be due to the amount of water available in the surrounding environment, and in the present study, a 95% relative humidity may have an affect the hydraulic setting reaction, resulting in a gain/loss of water volume. Complete hydration of some calcium-silicate based materials may take a year, however most hydration occurs during the first several days (Darvell & Wu, 2011). Under in vivo conditions, retrograde materials come into contact with apical tissue prior to complete hydration. When MTA is immersed in Hank's balanced salt solution (HBSS), the material exhibits an extended setting time (Camilleri, Formosa, & Damidot, 2013). The presence of phosphate ions and glucose in the HBSS solution retards the hydration of the cement (Ramachundran, 1992). Minimal Essential Media (MEM) also contains glucose, and prolonged setting times have been reported for ERRM and MTA in the presence of MEM and blood (Charland et al., 2013). In a saturated environment, hydration of the calcium-silicate based materials can cause expansion due to production of their by-products, gel hydrate phase and crystalline phase (Bentz et al., 2001). As previously mentioned, the formation of hydroxyapaptetite on the surface of these materials occurs in the

presence phosphate ions, and precipitation has been postulated to improve the seal due to the net expansion, as seen in an LVDT study with MTA (Gandolfi et al., 2009). Camillerili (2011) reported net expansion when W-MTA was exposed to HBSS after 28 days, compared to shrinkage observed at 100% humidity. Compared to Portland cement, the author postulated that the addition of bismuth oxide reduced the leaching of calcium ions from the hydration reactions, and this reduction may affect the material's dimensional stability (Camilleri, 2011). Storm et al. (2008) found greater expansion for W-MTA in HBSS compared to distilled water after 24 hours, 0.11 ± 0.03% and 0.08 ± 0.01% respectively. Under the same conditions, the authors found a decrease in expansion with G-MTA and they postulated this was due to a possible reaction with aluminoferrite. Similarly, Gandolfi et al. (2009) reported net expansion of W-MTA when immersed in distilled water, phosphate-buffering solution (PBS), 80% PBS/20% fetal bovine solution (FBS), and hexadecane. W-MTA showed greater expansion in PBS compared to distilled water, 0.77 ± 0.27% and 1.04 ± 0.25% respectively (Gandolfi et al., 2009). Camilleri and Mallia (2011) reported net shrinkage of W-MTA in 100% humidity and expansion in HBSS. In a SEM study by Shokouhinejad et al. (2014), marginal adaptation of ERRM-P to dentin was better than W-MTA after immersion in 7 days of PBS. Intensity mapping of W-MTA without cracks showed vector displacements approximately ranging from 1.2 to 2.5 μm with a trend of expansion in the periphery, as evident by the in arrow directions (Figure 8). Intensity mapping of ERRM-FS without cracks showed vector displacements approximately ranging from 1.5 to 2.0 μm with a similar direction of expansion (Figure 9). The displacement of W-MTA and ERRM-FS was smaller than gaps observed in the Shokouhinejad et al. (2014) study, 4.25 μm and 2.78 μm respectively. The mean linear expansion between the initial and final setting time, 240 minutes, for W-MTA without cracks (n=8) was 0.06 ± 0.36%, with a maximum expansion of 0.66 % (Table 5 & 8). Compared to the ERRM-FS without cracks (n=4), the mean linear expansion was 0.71 ± 0.19%, with a maximum expansion of 0.88 % (Table 5 & 7). Although W-

MTA without cracks was in compliance with the 0.1% maximum shrinkage requirements, ERRM-FS without cracks was not. For a material thickness of 100 μm, allotted displacement of 0.1 μm has not been proven to induce fractures.

The clinical relevance of microcracking can result in the recontamination the root canal system, and if the material does not fully cure under saturated conditions, erosion of the material could ensue leading to washout. In a study by Camilleri (2014), a gap of 1-2 μm was reported between Biodentine and dentin under dry conditions and when exposed to physiological solution, a void of 2 μm was observed. Intensity mapping of Biodentine showed vector displacements approximately ranging from 2 to 8 μm with a trend towards contraction, evident by the arrow directions (Figure 10). Although Biodentine was in compliance to the 1% maximum shrinkage requirements, a material thickness of 100 μm may be allowed 1 μm of displacement, which is large enough to allow bacterial penetration. In a SEM study by Camilleri et al.(2013) and Camilleri and Mallia (2011), MTA showed the presence of microcracks when exposed to HBSS and the authors speculated this was due to expansion. In the positive expansion group, two samples of Cavit exhibited cracking and its postulated that this was due to inadequate water content in the surrounding environment (Table 4). Within the confines of this experimental design, cracks were observed in W-MTA (n=2) and ERRM-FS (n=6), and the affect of cracking was significant. The mean linear expansion between the initial and final setting time, 240 minutes, for ERRM-FS with cracks (n=6) was 2.62 ± 1.22%, with a maximum expansion of 4.24% (Table 5 & 7). Compared to W-MTA with cracks (n=2), the mean linear expansion was almost double, 1.18 ± 0.27%, with a maximum expansion of 1.37 % (Table 5). After removing the cracks, the percentage changes for expansion for W-MTA and ERRM-FS were similar ($p=0.0008$), and ERRM-FS was significantly larger compared to W-MTA and Biodentine. Changes in ambient temperature and humidity produced cracks on material's surfaces in the LVDT study by Orstavik et al. (2001). In the present study, the cracks observed could have been

due to inadequate hydration, as cracks were evident in the positive control groups for expansion. The degree of hydration is greater for cements with finer particle sizes and requires less time to hydrate than coarser cements (Bentz et al., 2001). The chemical shrinkage of Portland cements are 10% by volume, compared to the physical shrinkage than can range from 0.01-0.1% (Bentz et al., 2001). Cracks observed in the W-MTA and ERRM-FS samples could be due to the initial expansion, due to hydration reactions, followed by contraction due to desiccation. The split mold design allowed unrestricted initial expansion in the direction perpendicular to the split only Constraints in the direction parallel to the split set up tensile stresses that fractured some of the specimens with large expansion. The clinical implication is that, if there are voids present within the filling, the unbalanced constraints would set up tensile stresses that could fracture the filling.

Dimensional stability of root-end filling materials can be influenced by the in vitro environment conditions during setting. Root-end filling materials are commonly encased in vivo by hard and soft tissue structures such as dentin, cementum, alveolar bone, obturation materials, and bodily fluids. Several studies have used laterally restricted molds to mimic this clinical situation and variations reported in the literature for the mean linear displacement could be due to the mold's size, the mold's material, technique for compacting specimens, experimental duration, and presence of available moisture. Under the conditions of this study, the hydroscopic expansion of ERRM-FS was significantly greater than that of W-MTA and control. The descending order of expansion was ERRM-FS, W-MTA, and Biodentine and thus, the null hypothesis was rejected for this present study. Consideration for further study would be to measure volumetric change using micro-CT on human teeth under simulated in vivo conditions. When immersed in physiological solutions, the charcoal carbon particles may be washed off and would limit the use of DIC analysis.

CONCLUSION

Following root-end resection, the purpose of a root-end filling material is to provide a seal to prevent the leakage of irritants into the periapical tissues and prevent egress of bacteria and inflammatory mediators in the apical tissues into the root canal system. The material's dimensional stability during setting can affect its marginal adaption to the cavity walls, where microscopic shrinkage can result in gaps and microscopic expansion can further close the interfaces *in vivo*. *In vitro,* hydroscopic shrinkage using DIC was observed for Biodentine, whereas expansion was seen for ERRM-FS and W-MTA, with the means being statistically significantly different ($p<0.0001$). The groups that complied with the maximum 1% shrinkage and 0.1% expansion requirement included Biodentine ($-0.01 \pm 0.21\%$) and W-MTA group, excluding the presence of cracks ($0.06 \pm 0.36\%$). ERRM-FS exceed the 0.1% expansion recommendations, with expansion in the overall ERRM-FS group and group without cracks measuring $1.86 \pm 1.34\%$ and $0.71 \pm 0.19\%$, respectively. In the present study, the occurrence of cracking was significant ($p<0.0001$), where more fractures were observed in premixed materials with large expansion (Cavit, ERRM-FS). Compared to the x-direction, constraints in the y-direction were always greater, which could set up tensile stresses capable of fracturing the filling materials.

REFERENCES

Adamo, H., Buruiana, R., Schertzer, L., & Boylan, R. (1999). A comparison of MTA, Super-EBA, composite, and amalgam as root-end filling materials using a bacterial microleakage model. *Int Endod J*, *32*, 197–203.

Al-Hezaimi, K., Naghshbandi, J., Oglesby, S., Simon, J., & Rotstein, I. (2005). Human saliva penetration of root canals obturated with two types of mineral trioxide aggregate cements. *J Endod*, *31*, 453–6.

Al Fouzan, K., Awadh, M., Badwelan, M., Gamal, A., Geevarghese, A., Babhair, S., … Rotstein, I. (2015). Marginal adaptation of mineral trioxide aggregate (MTA) to root dentin surface with orthograde/retrograde application techniques: A microcomputed tomographic analysis. *J Conserv Dent*, *18*(2), 109–13.

Andelin, W., Browning, D., Hsu, G., Roland, D., & Torabinejad, M. (2002). Microleakage of Resected MTA. *J Endod*, *28*(8), 573–4.

ANSI/ADA No. 57. (2000). Endodontic Sealing Materials. Chicago, IL: American Dental Association, Council of Scienctific Affairs.

Aqrabawi, J. (2000). Sealing ability of amalgam, Super EBA cement, and MTA when used as retrograde filling materials. *Br Dent J*, *188*, 266–8.

Asgary, S., Parirokh, M., Eghbal, M., & Brink, F. (2005). Chemical differences between white and gray mineral trioxide aggregate. *J Endod*, *31*, 101–103.

Barone, C., Dao, T., Basrani, B., Wang, N., & Friedman, S. (2010). Treatment Outcome in Endodontics : The Toronto Study-Phases 3, 4, and 5: Apical Surgery. *J Endod*, *36*(1), 28–35. https://doi.org/10.1016/j.joen.2009.09.001

Basturk, F., Nekoofar, M., Gunday, M., & Dummer, P. (2014). Effect of Various Mixing and Placement Techniques on the Flexural Strength and Porosity of Mineral Trioxide Aggregate. *J Endod*, *40*(3), 441–445. https://doi.org/10.1016/j.joen.2013.08.010

Bates, C., Carnes, D., & del Rio, C. (1996). Longitudinal sealing ability of mineral trioxide aggregate as a root-end filling material. *J Endod*, *22*, 575–8.

Belio-Reyes, I., Bucio, L., & Cruz-Chavez, E. (2009). Phase Composition of ProRoot Mineral Trioxide Aggregate by X-Ray Powder Diffraction. *J Endod*, *35*(6), 875–878. https://doi.org/10.1016/j.joen.2009.03.004

Bentz, D., & Aitcin, P. (2008). The Hidden Meaning of Water- Cement Ratio Distance between cement particles is fundamental. *Concrete Int*, (May), 51–54.

Bentz, D., Jensen, O., Hansen, K., Olesen, J., Stang, H., & Haecker, C. (2001). Influence of cement particle-size distribution on early age autogenous strains and stresses in cement-based materials. *J Am Ceram Soc*, *84*(1), 129–135.

Bernardi, A., Bortoluzzi, E., Felippe, W., Felippe, M., Wan, W., & Teixeira, C. (2017). Effects of the addition of nanoparticulate calcium carbonate on setting time , dimensional change , compressive strength , solubility and pH of MTA. *Int Endod J*, *50*(1), 97–105. https://doi.org/10.1111/iej.12594

Camilleri, J. (2007). Hydration mechanisms of mineral trioxide aggregate. *Int Endod J*, *40*, 462–470. https://doi.org/10.1111/j.1365-2591.2007.01248.x

Camilleri, J. (2008). Characterization of hydration products of mineral trioxide aggregate. *Int Endod J*, *41*(5), 408–417. https://doi.org/10.1111/j.1365-2591.2007.01370.x

Camilleri, J. (2011). Evaluation of the effect of intrinsic material properties and ambient conditions on the dimensional stability of white mineral trioxide aggregate and Portland cement. *J Endod*, *37*(2), 239–245. https://doi.org/10.1016/j.joen.2010.11.012

Camilleri, J., Formosa, L., & Damidot, D. (2013). The setting characteristics of MTA Plus in different environmental conditions. *Int Endod J*, *46*, 831–840. https://doi.org/10.1111/iej.12068

Camilleri, J., Grech, L., Galea, K., Keir, D., Fenech, M., Formosa, L., … Mallia, B. (2014).

Porosity and root dentine to material interface assessment of calcium silicate-based root-end filling materials. *Clin Oral Invest*, *18*, 1437–1446. https://doi.org/10.1007/s00784-013-1124-y

Camilleri, J., Kralj, P., Veber, M., & Sinagra, E. (2012). Characterization and analyses of acid-extractable and leached trace elements in dental cements. *Int Endod J*, *45*, 737–743. https://doi.org/10.1111/j.1365-2591.2012.02027.x

Camilleri, J., & Mallia, B. (2011). Evaluation of the dimensional changes of mineral trioxide aggregate sealer. *Int Endod J*, *44*(5), 416–424. https://doi.org/10.1111/j.1365-2591.2010.01844.x

Camilleri, J., Sorrentino, F., & Damidot, D. (2013). Investigation of the hydration and bioactivity of radiopacified tricalcium silicate cement, Biodentine and MTA Angelus. *Dent Mater*, *29*(5), 580–593. https://doi.org/10.1016/j.dental.2013.03.007

Carr, G. (1997). Ultrasonic root end preparation. *Dent Clin North Am*, *41*, 541–554.

Challacombe, S., Russell, M., Hawkes, J., Bergmeier, L., & Lehner, T. (1978). Passage of immunoglobulins from plasma to the oral cavity in rhesus monkeys. *Immunology*, *35*, 923–931.

Charland, T., Hartwell, G., Hirschberg, C., & Patel, R. (2013). An evaluation of setting time of mineral trioxide aggregate and endosequence root repair material in the presence of human blood and minimal essential media. *J Endod*, *39*(8), 1071–1072. https://doi.org/10.1016/j.joen.2013.04.041

Chen, C., Ho, C., Chen, C., Wang, W., & Ding, S. (2009). In vitro bioactivity and biocompatibility of dicalcium silicate cements for endodontic use. *J Endod*, *35*, 1154–7.

Chng, H., Islam, I., & Yap, A. (2005). Properties of a New Root-End Filling Material. *J Endod*, *31*(9), 665–668.

Coleman, N., Awosanya, K., & Nicholson, J. (2009). Aspects of the in vitro bioactivity of

hydraulic calcium (alumino) silicate cement. *J Biomed Mater Res A.*, *90*(1), 166–74. https://doi.org/10.1002/jbm.a.32070.

Coomaraswamy, K., Lumley, P., & Hofmann, M. (2007). Effect of Bismuth Oxide Radioopacifier Content on the Material Properties of an Endodontic Portland Cement – based (MTA-like) System. *J Endod*, *33*(3), 295–298. https://doi.org/10.1016/j.joen.2006.11.018

Craig, R., & Peyton, F. (1958). Elastic and mechanical properties of human dentin. *J Dent Res*, *37*, 710–8.

Dammaschke, T., Gerth, H., Zuchner, H., & Schafer, E. (2005). Chemical and physical surface and bulk material characterization of white ProRoot MTA and two Portland cements. *Dent Mater*, *21*, 731–738.

Darvell, B., & Wu, R. (2011). "MTA"-an Hydraulic Silicate Cement: review update and setting reaction. *Dent Mater*, *27*(5), 407–22.

De Bruyne, M., De Bruyne, R., Rosiers, L., & De Moor, R. (2005). Longitudinal study on microleakage of three root-end filling materials by the fluid transport method and by capillary flow porometry. *Int Endod J*, *38*, 129–36.

de Chevigny, C., Dao, T., Basrani, B., Marquis, V., Farzaneh, M., Abitbol, S., & Friedman, S. (2008). Treatment Outcome in Endodontics : The Toronto Study — Phase 4 : Initial Treatment. *J Endod*, *34*(3), 258–263. https://doi.org/10.1016/j.joen.2007.10.017

de Chevigny, C., Dao, T., Basrani, B., Marquis, V., Farzaneh, M., Abitbol, S., & Friedman, S. (2008). Treatment Outcome in Endodontics : The Toronto Study — Phases 3 and 4 : Orthograde Retreatment. *J Endod*, *34*(2), 131–137. https://doi.org/10.1016/j.joen.2007.11.003

De Deus, G., Camilleri, J., Primus, C., Duarte, M., & Bramante, C. (2014). Introduction to Mineral Trioxide Aggregate. In J. Camilleri (Ed.), *Mineral Trioxide Aggregate in Dentistry:*

From Preparation to Application (1st ed., pp. 1–18). Heidelberg: Springer.

Ding, S., Shie, M., & Wang, C. (2009). Novel fast-setting calcium silicate bone cements with high bioactivity and enhanced osteogenesis in vitro. *J Mater Chem*, *19*, 1183–90.

Fischer, E., Arens, D., & Miller, C. (1998). Bacterial leakage of mineral trioxide aggregate as compared with zinc-free amalgam, intermediate restorative material, and Super EBA as a root-end filling material. *J Endod*, *24*, 176–9.

Fogel, H., & Peikoff, M. (2001). Microleakage of root-end filling materials. *J Endod*, *24*, 456–8.

Fridland, M., & Rosado, R. (2003). Mineral trioxide aggregate (MTA) solubility and porosity with different water-to-powder ratios. *J Endod*, *29*(12), 814–7.

Friedman, S. (1991). Retrograde approaches in endodontic therapy. *Endod Dent Traumatol*, *7*, 97–107.

Friedman, S. (2005). The prognosis and expected outcome of apical surgery. *Endod Topics*, *11*(1), 219–262.

Gandolfi, M., Iacono, F., Agee, K., Siboni, F., Tay, F., Pashley, D., & Prati, C. (2009). Setting time and expansion in different soaking media of experimental accelerated calcium-silicate cements and ProRoot MTA. *Oral Surg Oral Med Oral Pathol Oral Radiol Endod*, *108*(6), e39–e45. https://doi.org/10.1016/j.tripleo.2009.07.039

Gandolfi, M., Taddei, P., Tinti, A., & Prati, C. (2010). Apatite-forming ability (bioactivity) of ProRoot MTA. *Int Endod J*, *23*, 917–929. https://doi.org/10.1111/j.1365-2591.2010.01768.x

Gondim, E., Zaia, A., Gomes, B., Ferraz, C., Teixeira, F., & Souza-Filho, F. (2003). Investigation of the marginal adaptation of root-end filling materials in root-end cavities prepared with ultrasonic tips. *Int Endod J*, *36*, 491–499.

Grech, L., Mallia, B., & Camilleri, J. (2013). Characterization of set Intermediate Restorative Material , Biodentine , Bioaggregate and a prototype calcium silicate cement for use as root-end filling materials. *Int Endod J*, *46*, 632–641. https://doi.org/10.1111/iej.12039

Ha, W., Bentz, D., Kahler, B., & Walsh, L. (2017). D90 : The Strongest Contributor to Setting Time in Mineral Trioxide Aggregate and Portland Cement. *J Endod*, *41*(7), 1146–1150. https://doi.org/10.1016/j.joen.2015.02.033

Hawley, M., Webb, T., & Goodell, G. (2010). Effect of Varying Water-to-Powder Ratios on the Setting Expansion of White and Gray Mineral Trioxide Aggregate. *J Endod*, *36*(8), 1377–1379. https://doi.org/10.1016/j.joen.2010.03.010

Herzog-Flores, D., Andrade, V., & Mendez, G. (2000). Physical chemical analysis of mineral trioxide aggregate (MTA) by X-rays diffraction, colorimetry and electronic microscopy. *Rev ADM*, *17*, 125–131.

Islam, I., Chng, H., & Yap, A. (2006). Comparison of the Physical and Mechanical Properties of MTA and Portland Cement. *J Endod*, *32*(3), 193–197. https://doi.org/10.1016/j.joen.2005.10.043

ISO 23317. (2014). Implants for surgery - In vitro evaluation for apatite-forming ability of implant materials.

ISO 6876. (2001). International Organization for Standardization 6876: Dental root canal sealing materials. *BS EN ISO 6876*.

Kakehashi, S., Stanley, H., & Fitzgerald, R. (1985). The effects of surgical exposures of dental pulps in germ-free and conventional laboratory rats. *Oral Surg Oral Med Oral Pathol Oral Radiol Endod*, *20*(3), 340–349.

Kanchanavasita, W., Pearson, G., & Anstice, H. (1995). Influence of humidity on dimensional stability of a range of ion-leachable cements. *Biomaterials*, *16*(12), 921–929.

Kim, S., & Kratchman, S. (2006). Modern Endodontic Surgery Concepts and Practice : A Review. *J Endod*, *32*(7), 601–623.

Kim, S., Pecora, G., & Rubinstein, R. (2001). *Comparison of traditional and microsurgery in endodontics. In: Color Atlas of Microsurgery in Endodontics*. (S. Kim, G. Pecora, & R.

Rubinstein, Eds.). Philadelphia: W.B. Saunders Company.

Kogan, P., He, J., Glickman, G., & Wantanabe, I. (2006). The Effects of Various Additives on Setting Properties of MTA. *J Endod*, *32*(6), 569–572. https://doi.org/10.1016/j.joen.2005.08.006

Komabayashi, T., & Spångberg, L. (2008). Comparative Analysis of the Particle Size and Shape of Commercially Available Mineral Trioxide Aggregates and Portland Cement : A Study with a Flow Particle Image Analyzer. *J Endod*, *34*(1), 94–8. https://doi.org/10.1016/j.joen.2007.10.013

Lamb, E., Loushine, R., Weller, R., Kimbrough, W., & Pashley, D. (2003). Effect of root resection on the apical sealing ability of mineral trioxide aggregate. *Oral Surg Oral Med Oral Pathol Oral Radiol Endod*, *95*(6), 732–5. https://doi.org/10.1067/moe.2003.98

Lau, A., Li, J., Heo, Y., & Fok, A. (2015). A study of polymerization shrinkage kinetics using digital image correlation. *Dent Mater*, *31*(4), 391–398. https://doi.org/10.1016/j.dental.2015.01.001

Lee, E. (2000). A new mineral trioxide aggregate root-end filling technique. *J Endod*, *26*(12), 764–5.

Li, J., Fok, A., Satterthwaite, J., & Watts, D. (2009). Measurement of the full-field polymerization shrinkage and depth of cure of dental composites using digital image correlation. *Dent Mater*, *25*, 582–588. https://doi.org/10.1016/j.dental.2008.11.001

Liu, W., & Chang, J. (2009). In vitro evaluation of gentamycin release from a bioactive tricalcium silicate bone cement. *Materials Science and Engineering: C*, *29*(8), 2486–92. https://doi.org/https://doi.org/10.1016/j.msec.2009.07.015

Luyckx, T., Verstraete, M., Roo, K., Waele, W., Bellemans, J., & Victor, J. (2014). Digital image correlation as a tool for three-dimensional strain analysis in human tendon tissue. *J Exp Orthop*, *1*(7), 1–9. https://doi.org/10.1186/s40634-014-0007-8

Ma, J., Shen, Y., Stojicic, S., & Haapasalo, M. (2011). Biocompatibility of Two Novel Root Repair Materials. *J Endod*, *37*(6), 793–798. https://doi.org/10.1016/j.joen.2011.02.029

Maltezos, C., Glickman, G., Ezzo, P., & He, J. (2006). Comparison of the sealing of Resilon, Pro Root MTA, and Super-EBA as root-end filling materials: a bacterial leakage study. *J Endod*, *32*(324–7).

Miletic, V., Manoilovic, D., Milosevic, M., Mitrovic, N., Stankovic, T., & Maneski, T. (2011). Analysis of local shrinkage patterns of self-adhering and flowable composites using 3D digital image correlation. *Quintessence Int*, *42*(9), 797–804.

Moinzadeh, A., Portoles, C., Wismayer, P., & Camilleri, J. (2016). Bioactivity Potential of EndoSequence BC RRM Putty. *J Endod*, *42*(4), 615–621. https://doi.org/10.1016/j.joen.2015.12.004

Moller, A., Fabricius, L., Dahlen, G., Ohman, A., & Heyden, G. (1981). Influence on periapical tissues of indigenous oral bacteria and necrotic pulp tissue in monkeys. *Scand J Dent Res*, *89*, 475–84.

Montellano, A., Schwartz, S., & Beeson, T. (2006). Contamination of tooth-colored mineral trioxide aggregte used as a root-end filling material: a bacterial leakage study. *J Endod*, *32*, 452–5.

Material Safety Data Sheet (MSDS). (2002). *ProRoot MTA™ (mineral trioxide aggregate) Root Canal Repair Material*. Tulsa, OK: Dentsply Tulsa Dental.

Material Safety Data Sheet (MSDS). (2008). Filtek LS™ Technique Guide Instructions. St. Paul, MN: 3M ESPE.

Material Safety Data Sheet (MSDS). (2010). *Biodentine™ Activate Biosilicate Technology™*. St. Maur-des-Fossés, France: Septodont.

Material Safety Data Sheet (MSDS). (2014). BC RRM-Fast Set Putty ™ Material. Savanah, GA: Brasseler.

Nair, P. (2004). Pathogenesis of apical periodontitis and the causes of endodontic failures. *Crit Rev Oral Biol Med*, *15*(6), 348–381.

Ono, K., & Matsumoto, K. (1992). The physical properties of a new sealing cement. *Int Endod J*, *25*, 130–133.

Orstavik, D., Nordahl, I., & Tibballs, J. (2001). Dimensional change following setting of root canal sealer materials. *Dent Mater*, *17*, 512–519.

Parirokh, M., & Torabinejad, M. (2010). Mineral trioxide aggregate: a comprehensive literature review—Part I: chemical, physical, and antibacterial properties. *J Endod*, *36*(1), 16–27.

Primus, C. (2017). MTA Phases by XRD. In: Bioactive Dental Cements, Research on Quick-Set Material (Presentation, University of Minnesotta, 2017). Primus, C.

Ramachundran, V. (1992). Interaction of admixtures in the cement-water system. In A. Paillere & F. Spon (Eds.), *Application of admixtures in concret* (1st, Rilem ed., pp. 1–14). London: CRC Press.

Ravichandra, P., Vemisetty, H., Reddy, S., Ramkiran, D., Krishna, M., & Malathi, G. (2014). Comparative Evaluation of Marginal Adaptation of Biodentine TM and Other Commonly Used Root End Filling Materials- An In vitro Study. *J Clin Diagn Res*, *8*(3), 243–245. https://doi.org/10.7860/JCDR/2014/7834.4174

Roberts, H., Toth, J., Berzins, D., & Charlton, D. (2008). Mineral trioxide aggregate material use in endodontic treatment: A review of the literature. *Dent Mater*, *24*(2), 149–164. https://doi.org/10.1016/j.dental.2007.04.007

Roy, C., Heansonne, B., & Gerrets, T. (2001). Effect of an acid environment on leakage of root-end filling materials. *J Endod*, *27*, 7–8.

Sarkar, N., Caicedo, R., Ritwik, P., Moiseyeva, R., & Kawashima, I. (2005). Physicochemical Basis of the Biologic Properties of Mineral Trioxide Aggregate. *J Endod*, *31*(2), 97–100.

Scheere, S., Steiman, H., & Cohen, J. (2004). A comparative evaluation of three root-end filling

materials: an in vitro leakage study using Prevotella nigrescens. *J Endod*, *30*, 782–4.

Schilder, H. (1967). Filling Root Canals in Three Dimensioins. *Dent Clin North Am*, *11*, 723–744.

Schilder, H. (1974). Cleaning and shaping the root canal. *Dent Clin North Am*, *18*(2), 269–296.

Septodont. (2010). Biodentine™ Scientific File Activated Biosilicate Technology™.

Shokouhinejad, N., Nekoofar, M., Ashoftehyazdi, K., Zahraee, S., & Khoshkhounejad, M. (2014). Marginal Adaptation of New Bioceramic Materials and Mineral Trioxide Aggregate : A Scanning Electron Microscopy Study. *Iran Endod J.*, *9*(2), 144–148.

Stabholz, A., Shani, J., Friedman, S., & Abed, J. (1985). Marginal Adaptation of Retrograde Fillings and Its Correlation with Sealability. *J Endod*, *11*(5), 218–223.

Stefopoulos, S., Tsatsas, D., Kerezoudis, N., & Eliades, G. (2008). Comparative in vitro study of the sealing efficiency of white vs grey ProRoot mineral trioxide aggregate formulas as apical barriers. *Dent Traumatol*, *24*(2), 207–13.

Storm, B., Eichmiller, F., Tordik, P., & Goodell, G. (2008). Setting Expansion of Gray and White Mineral Trioxide Aggregate and Portland Cement. *J Endod*, *34*(1), 80–82. https://doi.org/10.1016/j.joen.2007.10.006

Sundqvist, G., & Figdor, D. (2003). Life as an endodontic pathogen. Ecological differences between the untreated and root-filled root canals. *Endod Topics*, *6*, 3–28.

Torabinejad, M., Eby, W., & Naidorf, I. (1985). Inflammatory and Immunological Aspects of the Pathogenesis of Human Periapical Lesions. *J Endod*, *11*(4), 479–488.

Torabinejad, M., Falah Rastegar, A., Kettering, J., & Pitt Ford, T. (1995). Bacterial leakage of mineral trioxide aggregate as a root end filling material. *J Endod*, *21*, 109–112.

Torabinejad, M., Higa, R., McKendry, D., & Pitt Ford, T. (1993). Dye leakage of four root end filling materials: effect of blood contamination. *J Endod*, *20*, 159–63.

Torabinejad, M., Hong, C., McDonald, F., & Pitt Ford, T. (1995). Physical and chemical

properties of a new root-end filling material. *J Endod*, *21*(7), 349–353. https://doi.org/10.1016/s0099-2399(06)80967-2

Torabinejad, M., & Parirokh, M. (2010). Mineral trioxide aggregate: a comprehensive literature review—part II: leakage and biocompatibility investigations. *J Endod*, *36*(2), 16–27.

Torabinejad, M., & Pitt Ford, T. (1996). Root end filling materials : a review. *Endod Dent Traumatol*, *12*, 161–179.

Torabinejad, M., Smith, P., Kettering, J., & Pitt Ford, T. (1995). Comparative Investigation of Marginal Adaptation of Mineral Trioxide Aggregate and Other Commonly Used Root-End Filling Materials. *J Endod*, *21*(6), 295–299.

Torabinejad, M., Watson, T., & Pitt Ford, T. (1993). Sealing ability of a mineral trioxide aggregate when used as a root end filling material. *J Endod*, *19*(12), 591–595. https://doi.org/10.1016/S0099-2399(06)80271-2

Tran, D., He, J., Glickman, G., & Woodmansey, K. (2016). Comparative Analysis of Calcium Silicate – based Root Filling Materials Using an Open Apex Model. *J Endod*, *42*(4), 654–658. https://doi.org/10.1016/j.joen.2016.01.015

Tselnik, M., Baumgartner, J., & Marshall, J. (2004). Bacterial leakage with mineral trioxide aggregate or a resin-modified glass-ionomer used as a coronal barrier. *J Endod*, *30*, 782–4.

Valois, C., & Costa, E. (2004). Influence of the thickness of mineral trioxide aggregate on the sealing ability of root-end fillings in vitro. *Oral Surg Oral Med Oral Pathol Oral Radiol Endod*, *97*, 108–11.

von Arx, T., Penarrocha, M., & Jensen, S. (2010). Prognostic Factors in Apical Surgery with Root-end Filling: A Meta-Analysis. *J Endod*, *36*(6), 957–973. https://doi.org/10.1016/j.joen.2010.02.026

Widerman, F., Eames, W., & Serene, T. (1971). The physical and biologic properties of Cavit. *JADA*, *82*(2), 378–382. https://doi.org/10.14219/jada.archive.1971.0068

Wiltbank, K., Schwartz, S., & Schindler, W. (2007). Effect of Selected Accelerants on the Physical Properties of Mineral Trioxide Aggregate and Portland Cement. *J Endod*, *33*(10), 1235–1238. https://doi.org/10.1016/j.joen.2007.06.016

Wu, M., Kontakiotis, E., & Wesselink, P. (1998). Long-term seal provided by some root-end filling materials. *J Endod*, *24*, 557–60.

Xavier, C., Weismann, R., de Oliveira, M., Demarco, F., & Pozza, D. (2005). Root-end filling materials: apical microleakage and marginal adaptation. *J Endod*, *31*(7), 539–42.

Yatsushiro, J., Baumgartner, J., & Tinkle, J. (1998). Longitudinal study of the microleakage of two root-end filling materials using a fluid conductive system. *J Endod*, *24*, 716–9.

Zedler, A. (2016). *Dimensional Changes of ProRoot white Mineral Trioxide Aggregate , EndoSequence Root Repair Material , and Biodentine During Setting Using Digital Image Correlation*. (Master's Thesis, University of Minnesota, 2016). Retrieved from http://hdl.handle.net/11299/183293.

Zhang, D., & Arola, D. (2004). Applications of digital image correlation to biological. *J Biomed Opt*, *9*(4), 691–699. https://doi.org/10.1117/1.1753270

APPENDIX

Group	#	Exx	Eyy	2D%Strain	Crack	Avg Strain	Avg Strain (+ Crack)	Avg Strain (- Crack)
Biodentine	1	-0.3018	0.2045	0.1445		-0.0119	0.0000	-0.0119
	2	-0.0685	-0.2018	-0.2703				
	3	-0.0026	0.0439	0.0412				
	4	0.0880	-0.1978	-0.1099				
	5	0.3292	-0.0575	0.2717				
	6	-0.0556	0.0001	-0.0555				
	7	-0.3078	0.0066	-0.3013				
	8	0.0702	0.1648	0.2350				
	9	0.2645	-0.1116	0.1529				
	10	-0.1967	-0.0442	-0.2275				
ERRM	1	0.5275	0.1123	0.6398		1.8557	2.6195	0.7099
	2	0.5091	-0.0315	0.4775				
	3	0.3846	0.7565	1.1411	✔			
	4	0.9928	0.5506	1.5434	✔			
	5	0.5482	0.2922	0.8403				
	6	3.5067	0.2543	3.7609	✔			
	7	1.6147	0.6656	2.2803	✔			
	8	2.4115	0.3389	2.7504	✔			
	9	4.1028	0.1381	4.2409	✔			
	10	0.7351	0.1469	0.8820				
MTA	1	-0.1524	-0.0708	-0.2232		0.2872	1.1767	0.0649
	2	0.3283	0.3342	0.6625				
	3	-0.0963	0.1065	0.0102				
	4	0.6184	0.3642	0.9826	✔			
	5	-0.0336	-0.3572	-0.3909				
	6	0.1827	0.0203	0.2030				
	7	0.2793	0.1307	0.4100				
	8	-	-	-0.2752				

		0.1281	0.1471					
	9	1.1717	0.1991	1.3708	✔			
	10	0.0047	0.1179	0.1225				
Composite	1	-0.7303	-0.3947	-1.1251		-1.1433	0.0000	-1.1433
	2	-0.7169	-0.4814	-1.1981				
	3	-0.6640	-0.4426	-1.1066				
Cavit	1	1.4411	1.4491	2.8902		4.1992	4.8537	2.8902
	2	4.1228	1.5316	5.6544	✔			
	3	2.8704	1.1826	4.0529	✔			
Empty	1	-0.3149	0.3873	0.0720		0.0412	0.0000	0.0412
	2	-0.2734	0.2838	0.0104				

Table 10: The mean strain in Exx, Eyy, and two-dimensions for each sample in the experimental groups